Boundary effects on the local density of states of one-dimensional Mott insulators and charge density wave states

Dirk Schuricht,[1,2,*] Fabian H. L. Essler,[3] Akbar Jaefari,[4] and Eduardo Fradkin[4]

[1]*Institute for Theory of Statistical Physics, Rheinisch-Westfälische Technische Hochschule (RWTH) Aachen, D-52056 Aachen, Germany*

[2]*Jülich Aachen Research Alliance (JARA)–Fundamentals of Future Information Technology*

[3]*The Rudolf Peierls Centre for Theoretical Physics, University of Oxford, 1 Keble Road, Oxford OX1 3NP, UK*

[4]*Department of Physics, University of Illinois at Urbana-Champaign, 1110 West Green Street, Urbana, Illinois 61801-3080, USA*

(Received 29 September 2010; published 13 January 2011)

We determine the local density of states (LDOS) for spin-gapped one-dimensional charge density wave (CDW) states and Mott insulators in the presence of a hard-wall boundary. We calculate the boundary contribution to the single-particle Green function in the low-energy limit using field theory techniques and analyze it in terms of its Fourier transform in both time and space. The boundary LDOS in the CDW case exhibits a singularity at momentum $2k_F$, which is indicative of the pinning of the CDW order at the impurity. We further observe several dispersing features at frequencies above the spin gap, which provide a characteristic signature of spin-charge separation. This demonstrates that the boundary LDOS can be used to infer properties of the underlying *bulk* system. In the presence of a boundary magnetic field, midgap states localized at the boundary emerge. We investigate the signature of such bound states in the LDOS. We discuss the implications of our results for scanning tunneling microscopy experiments on quasi-one-dimensional systems such as two-leg ladder materials like $Sr_{14}Cu_{24}O_{41}$. By exchanging the roles of charge and spin sectors, all our results directly carry over to the case of one-dimensional Mott insulators.

DOI: 10.1103/PhysRevB.83.035111 PACS number(s): 68.37.Ef, 71.10.Pm, 72.80.Sk

I. INTRODUCTION

Scanning tunneling microscopy (STM) and spectroscopy (STS) methods have proved to be a useful tool for studying strongly correlated electron systems such as carbon nanotubes,[1] high-temperature superconductors (HTSCs),[2–5] and rare-earth compounds.[6] STM experiments measure the tunneling current I between the sample and the STM tip as a function of its position x and the applied voltage V. This current can be expressed in terms of the local densities of states (LDOS) in the sample $N(E,x)$ and the tip $N_{\rm tip}(E)$ as[5]

$$I(V,x) \propto \int dE\,[f(E-eV)-f(E)]\,N_{\rm tip}(E-eV)\,N(E,x), \tag{1}$$

where $f(E)$ denotes the Fermi function. Assuming a structureless density of states in the tip, $N_{\rm tip} = \text{const}$, this gives the following expression for the local tunneling conductance:

$$\frac{dI(V,x)}{dV} \propto \int dE\, f'(E-eV)\,N(E,x). \tag{2}$$

Equation (2) shows that the tunneling conductance is proportional to the thermally smeared $N(E,x)$ of the sample at the position of the tip. A nontrivial spatial dependence of the LDOS arises in presence of impurities. These break translational invariance and lead to a modification of the LDOS in their vicinity, from which one can infer characteristic properties of the *bulk* state of matter as well as the nature of its electronic excitations. Spatial modulations of the LDOS can be analyzed in terms the Fourier transform of the tunneling conductance. It follows from Eq. (2) that this quantity is directly proportional to the corresponding Fourier transform of the LDOS, $N(E,Q)$. This method of analyzing STM data was used very successfully[3] to study quasiparticle interference in $Bi_2Sr_2CaCu_2O_{8+\delta}$. The spin dependence of the LDOS has also been investigated using magnetic tips.[7] Theoretical studies of STS have focused, in particular, on Luttinger liquids[8,9] and HTSCs.[9–11] In the Luttinger liquid case an impurity has the same effects at low energies as a physical boundary,[12] which motivated studies of the LDOS in the vicinity of a chain end. The case of strongly correlated one-dimensional (1D) systems with spin or charge gaps is of considerable interest as well and pertains to quasi-1D charge density wave (CDW) systems[13] and Mott insulators,[14,15] carbon nanotubes,[16] (doped) two-leg ladder materials,[17,18] and the stripe phases of HTSCs.[19] Compared to the Luttinger liquid case, the presence of an interaction-induced gap makes these problems much more difficult to treat theoretically. In the following we determine the LDOS for the low-energy limit of 1D CDW states and Mott insulators in the presence of a single boundary. The latter can be thought of as arising as the result of the presence of a strong potential impurity. Alternatively, one can imagine inducing a boundary in a two-tip STM setup, where the first tip is used to induce a boundary by applying a high voltage and the LDOS is then measured with the second tip. A short summary of our results has appeared previously.[20]

The outline of this paper is as follows: in Sec. II we present the field theory limit of 1D CDW states and Mott insulators in the presence of a single boundary. In Sec. III we summarize our results for the single-particle Green function. These are then used to determine the Fourier transform $N_\sigma(E,Q)$ of the local density of states for hard-wall boundary conditions in Sec. IV. Signatures of spin and charge excitations visible in $N_\sigma(E,Q)$ are discussed in some detail. The effects of more general boundary conditions, including the formation of boundary bound states, are described in Sec. V. Section VI deals with the

effects of finite temperatures, and implications of our results for STM experiments are discussed in Sec. VII. The technical details of our calculations are presented in several appendixes.

II. THE MODEL

Our analysis of the LDOS is based on the continuum description of certain 1D CDW states and Mott insulators. The resulting quantum field theory for both cases is known as the U(1) Thirring model[21] (with two "flavors"). The latter is known to arise as the effective low-energy description of a number of lattice models of spin-1/2 electrons, as we discuss next.

(1) Half-filled repulsive Hubbard model:[22] This is the standard model for single-band 1D Mott insulators. The Hamiltonian is of the form

$$H = -t\sum_{j,\sigma}[c^\dagger_{j,\sigma}c_{j+1,\sigma} + c^\dagger_{j+1,\sigma}c_{j,\sigma}] + U\sum_j\left(n_{j,\uparrow}-\frac{1}{2}\right)\left(n_{j,\downarrow}-\frac{1}{2}\right), \tag{3}$$

where $n_{j,\sigma} = c^\dagger_{j,\sigma}c_{j,\sigma}$ and $n_j = n_{j,\uparrow} + n_{j,\downarrow}$ are electron number operators and $U > 0$.

(2) One-dimensional Holstein model:[23] The Holstein model provides an example of an incommensurate CDW state and describes a partially filled band of spin-1/2 electrons coupled to dispersionless phonons of frequency $\omega_0 = \sqrt{\frac{k}{M}}$:

$$H = -t\sum_{j,\sigma}[c^\dagger_{j,\sigma}c_{j+1,\sigma} + c^\dagger_{j+1,\sigma}c_{j,\sigma}] + \sum_j\left[\frac{P_j^2}{2M} + \frac{k}{2}Q_j^2\right] - \lambda\sum_{j,\sigma}Q_j n_{j,\sigma}. \tag{4}$$

Integrating out the phonons induces a retarded attractive electron-electron interaction. In the limit $t \ll \omega_0$ the retardation effects can be neglected, leading to an effective *attractive* Hubbard model with $U \propto -\lambda^2$.

(3) Su-Schrieffer-Heeger model:[24] A second example of an incommensurate CDW state is provided by the Su-Schrieffer-Heeger model, which describes a partially filled band of spin-1/2 electrons coupled to dispersing phonons:

$$H = -\sum_{j,\sigma}[t-\lambda(Q_{j+1}-Q_j)][c^\dagger_{j,\sigma}c_{j+1,\sigma} + c^\dagger_{j+1,\sigma}c_{j,\sigma}] + \sum_j\left[\frac{P_j^2}{2M} + \frac{k}{2}[Q_{j+1}-Q_j]^2\right]. \tag{5}$$

Taking the continuum limit of Eq. (5) (which describes the behavior at low frequencies, $\omega \lesssim t$), it was shown by Fradkin and Hirsch[25] that the regime of high phonon frequencies $t \ll \omega_0 = \sqrt{\frac{k}{M}}$ is described by the U(1) Thirring model.[21,26]

In all three cases a continuum description of the low-energy electronic degrees of freedom is obtained by considering only the modes in the vicinity of the Fermi points $\pm k_F$. The lattice electron annihilation operators are expressed in terms of slowly varying right- and left-moving Fermi fields as

$$\frac{c_{j,\sigma}}{\sqrt{a_0}} \to \Psi_\sigma(x) = e^{ik_F x}R_\sigma(x) + e^{-ik_F x}L_\sigma(x), \tag{6}$$

where a_0 is the lattice spacing, $x = ja_0$, and $\sigma = \uparrow, \downarrow$ labels the spin. In the bulk the fields R_σ and L_σ are bosonized according to

$$R^\dagger_\sigma(\tau,x) = \frac{\eta_\sigma}{\sqrt{2\pi}}\exp\left(\frac{i}{2}\phi_c(\tau,x)\right)\exp\left(\frac{i}{2}f_\sigma\phi_s(\tau,x)\right), \tag{7}$$

$$L^\dagger_\sigma(\tau,x) = \frac{\eta_\sigma}{\sqrt{2\pi}}\exp\left(-\frac{i}{2}\bar\phi_c(\tau,x)\right)\exp\left(-\frac{i}{2}f_\sigma\bar\phi_s(\tau,x)\right), \tag{8}$$

where the Klein factors η_σ satisfy anticommutation rules $\{\eta_\sigma,\eta'_\sigma\} = 2\delta_{\sigma\sigma'}$ and $f_\uparrow = 1 = -f_\downarrow$. Fields ϕ_a and $\bar\phi_a$ are the chiral components of the canonical Bose fields Φ_a and their dual fields Θ_a:

$$\Phi_a = \phi_a + \bar\phi_a, \quad \Theta_a = \phi_a - \bar\phi_a, \quad a = c,s. \tag{9}$$

In the bulk the Hamiltonian density then can be cast in the spin-charge separated form:

$$\mathcal{H}(x) = \sum_{a=c,s}\mathcal{H}_a(x),$$

$$\mathcal{H}_a = \frac{v_a}{16\pi}\left[\frac{1}{K_a^2}(\partial_x\Phi_a)^2 + K_a^2(\partial_x\Theta_a)^2\right] - \frac{g_a}{(2\pi)^2}\cos\Phi_a. \tag{10}$$

The charge and spin velocities $v_{c,s}$, Luttinger parameters $K_{c,s}$, and coupling constants $g_{c,s}$ are functions of the hopping integrals and interaction strengths defining the underlying microscopic model. The cases just discussed correspond to the following parameter regimes.

(1) Mott insulators: As a result of repulsive electron-electron interactions, we have $v_c > v_s$ and $K_c < 1$. The $\cos\Phi_c$ perturbation in the charge sector is relevant and opens up a gap. The $\cos\Phi_s$ interaction in the spin sector is marginally irrelevant and flows to 0 under the renormalization group. We therefore neglect it in the following.

(2) Electron-phonon systems: At low energies electron-phonon coupling induces an attractive electron-electron interaction, which results in $v_s > v_c$ and $K_c > 1 > K_s$. The $\cos\Phi_c$ term is irrelevant, while the $\cos\Phi_s$term is relevant [marginally relevant in the spin-SU(2) symmetric case $K_s = 1$] and opens up a gap in the spin sector.

In both cases we end up with a spin-charge separated theory of a gapless Luttinger liquid and a sine-Gordon model.

We now imagine a strong, local potential to be present. It is well known from the work of Kane and Fisher[12] that the coupling to the impurity is *relevant*, leading to a crossover at a characteristic dynamical energy (and temperature) scale called "T_K," below which the system is effectively cut into two disconnected parts, and to a pinning of the CDW. This potential could be due to a strong potential impurity or an STM tip. We model the strong impurity potential by a boundary condition on the continuum electron field:

$$\Psi_\sigma(x=0) = 0. \tag{11}$$

An important physical consequence of the pinning of the CDW at the impurity (or boundary) is the development of an *induced static CDW order* in this (effectively) quantum critical system. This induced static CDW order, often referred to[27] as a "Friedel oscillation," leads to nondispersive features in the LDOS[9] that can be detected in STM and STS experiments.

Our effective low-energy Hamiltonian in the CDW case (in the case of a Mott insulator the roles of spin and charge sectors are interchanged) then becomes

$$H = \sum_{a=\mathrm{c,s}} H_a, \tag{12}$$

$$H_\mathrm{c} = \frac{v_\mathrm{c}}{16\pi}\int_{-\infty}^{0} dx \left[\frac{1}{K_\mathrm{c}^2}(\partial_x \Phi_\mathrm{c})^2 + K_\mathrm{c}^2(\partial_x \Theta_\mathrm{c})^2\right], \tag{13}$$

$$H_\mathrm{s} = \frac{v_\mathrm{s}}{16\pi}\int_{-\infty}^{0} dx \left[\frac{1}{K_\mathrm{s}^2}(\partial_x \Phi_\mathrm{s})^2 + K_\mathrm{s}^2(\partial_x \Theta_\mathrm{s})^2\right] - \frac{g_\mathrm{s}}{(2\pi)^2}\int_{-\infty}^{0} dx\, \cos\Phi_\mathrm{s}, \tag{14}$$

where the Bose fields are subject to the hard-wall boundary conditions (we consider more general boundary conditions in Sec. V),

$$\Phi_{\mathrm{c,s}}(x=0) = 0. \tag{15}$$

In Appendix A we argue that a weak potential impurity renormalizes to strong coupling even for moderate attractive interactions, suggesting that this situation too can be modeled in terms of the boundary conditions, Eq. (15). We note that our starting point, Eqs. (12)–(15), differs from the model considered in Ref. 28, where the impurity couples only to the gapless charge sector.

The charge sector, Eq. (13), describes gapless collective charge excitations propagating with velocity v_c, which carry charge $\mp e$ and are commonly referred to as holons and antiholons, respectively. On the other hand, the spin excitations or spinons are described by the sine-Gordon model on the half-line, Eq. (14), which is known to be integrable for quite general boundary conditions.[29,30] In the regime $K_\mathrm{s} > 1/\sqrt{2}$ the elementary bulk excitations are gapped solitons and antisolitons, which correspond to up- and down-spin spinons, respectively. For $K_\mathrm{s} < 1/\sqrt{2}$, propagating breather (soliton-antisoliton) bound states occur as well. At the Luther-Emery point (LEP) $K_\mathrm{s} = 1/\sqrt{2}$, the spin sector is equivalent to a free massive Dirac fermion.[31] The exact bulk scattering matrix was first derived by Zamolodchikov;[32] the boundary reflection matrices of solitons and antisolitons[29] and breathers[33] were derived by Ghoshal and Zamolodchikov. We restrict ourselves to the regime $K_\mathrm{s} \geqslant 1/\sqrt{2}$ throughout, which implies that no breathers exist.

The lattice models already discussed give rise to the simplest kind of 1D CDW state/Mott insulator. More complicated versions arise in strongly correlated two- and three-leg ladder systems.[19,34] In these systems, even though electron interactions are strongly repulsive, a Mott state with a finite (and typically large) spin gap is found for a range of dopings close to half-filling. While the precise description of the spin sector for two-leg ladders is considerably more complicated,[35] we expect our calculation to capture important qualitative features.

III. GREEN FUNCTION

The central object of our study is the time-ordered Green function in Euclidean space,

$$G_{\sigma\sigma'}(\tau,x_1,x_2) = -\langle 0_\mathrm{b}|\, \mathcal{T}_\tau\, \Psi_\sigma(\tau,x_1)\, \Psi^\dagger_{\sigma'}(0,x_2)\, |0_\mathrm{b}\rangle\,, \tag{16}$$

where $|0_\mathrm{b}\rangle$ is the ground state of Eq. (12) in the presence of the boundary and $\tau = \mathrm{i}t$ denotes imaginary time. The spin takes the values $\uparrow$ and $\downarrow$. At low energies the linearization around the Fermi points yields the decomposition

$$G_{\sigma\sigma'} = e^{\mathrm{i}k_\mathrm{F}(x_1-x_2)}\, G^{RR}_{\sigma\sigma'} + e^{-\mathrm{i}k_\mathrm{F}(x_1-x_2)}\, G^{LL}_{\sigma\sigma'} + e^{\mathrm{i}k_\mathrm{F}(x_1+x_2)}\, G^{RL}_{\sigma\sigma'} + e^{-\mathrm{i}k_\mathrm{F}(x_1+x_2)}\, G^{LR}_{\sigma\sigma'}, \tag{17}$$

where, for example, $G^{RL}_{\sigma\sigma'} = -\langle 0_\mathrm{b}|\, \mathcal{T}_\tau\, R_\sigma(\tau,x_1)\, L^\dagger_{\sigma'}(0,x_2)\, |0_\mathrm{b}\rangle$. As we are interested in the LDOS, we ultimately want to set $x_1 = x_2$. Here we calculate the spatial Fourier transform of the LDOS, as physical properties can be more easily identified. In momentum space the RL and LR contributions occur in a different region ($Q \approx \pm 2k_\mathrm{F}$) compared to the RR and LL parts ($Q \approx 0$). In the absence of a boundary we have $G^{RL}_{\sigma\sigma'} = G^{LR}_{\sigma\sigma'} = 0$ as the charge parts of these Green functions vanish. In the presence of a boundary, left and right sectors are coupled and the Fourier transform of the Green function, Eq. (17), concomitantly acquires a nonzero component at $Q \approx \pm 2k_\mathrm{F}$, which provides a particularly clean way of investigating boundary effects. For this reason we first focus on the $2k_\mathrm{F}$ part of the Green function and then study the low-momentum regime.

The Green function $G^{RL}_{\sigma\sigma'}$ factorizes into a product of correlation functions in the spin and charge sectors. The charge part can be determined by standard methods[36–38] (see Appendix B). On the other hand, the integrability of the sine-Gordon model on the half-line, Eq. (14), enables us to calculate correlation functions in the spin sector using the boundary-state formalism introduced by Ghoshal and Zamolodchikov[29] together with a form-factor expansion.[39–44] As we show in Appendix C the leading terms in this expansion yield ($\tau > 0$, $x_1 < x_2$)

$$G^{RL}_{\sigma\sigma'}(\tau,x_1,x_2) = g_\mathrm{c}(\tau,x_1,x_2)\, g_\mathrm{s}(\tau,x_1,x_2), \tag{18}$$

$$g_\mathrm{c}(\tau,x_1,x_2) = -\frac{\delta_{\sigma\sigma'}}{2\pi}\frac{1}{(v_\mathrm{c}\tau - 2\mathrm{i}R)^a}\frac{1}{(v_\mathrm{c}\tau + 2\mathrm{i}R)^b} \times \left[\frac{4x_1x_2}{(v_\mathrm{c}\tau - \mathrm{i}r)(v_\mathrm{c}\tau + \mathrm{i}r)}\right]^c, \tag{19}$$

$$g_\mathrm{s}(\tau,x_1,x_2) = Z_1\, e^{\mathrm{i}\frac{\pi}{4}}\left[\frac{1}{\pi}\, K_0\big(\Delta\sqrt{\tau^2 + r^2/v_\mathrm{s}^2}\big) + \int_{-\infty}^{\infty}\frac{d\theta}{2\pi}\, K\left(\theta + \mathrm{i}\frac{\pi}{2}\right) \times\, e^{\theta/2}\, e^{2\mathrm{i}\frac{\Delta}{v_\mathrm{s}}R\sinh\theta}\, e^{-\Delta\tau\cosh\theta} + \cdots\right], \tag{20}$$

where $g_{c,s}$ are the contributions of the charge and spin sectors, respectively. Here K_0 is a modified Bessel function and the center-of-mass coordinates are $R = (x_1 + x_2)/2 < 0$ and $r = x_1 - x_2 < 0$. The normalization constant Z_1 was obtained in Ref. 42. At the LEP[45] and the SU(2) invariant point the boundary reflection amplitude $K(\theta)$ is given by

$$\begin{aligned} K(\theta) &= \mathrm{i}\tanh\frac{\theta}{2} \quad \text{for} \quad K_s = \frac{1}{\sqrt{2}}, \\ K(\theta) &= -\frac{\theta}{\pi^{3/2}}\frac{\Gamma\left(\frac{\mathrm{i}\theta}{\pi}\right)\Gamma\left(\frac{3}{4}-\frac{\mathrm{i}\theta}{2\pi}\right)}{\Gamma\left(\frac{5}{4}+\frac{\mathrm{i}\theta}{2\pi}\right)}2^{-\frac{\mathrm{i}}{\pi}\theta} \\ &\quad \times \sinh\frac{\theta}{2} \quad \text{for} \quad K_s = 1. \end{aligned} \tag{21}$$

The expressions for general values of K_s can be found in Refs. 29, 46, and 47. The exponents in the charge sector are related to the Luttinger parameter by

$$\begin{aligned} a = \frac{1}{8}\left(K_c + \frac{1}{K_c}\right)^2, \quad b = \frac{1}{8}\left(K_c - \frac{1}{K_c}\right)^2, \\ c = \frac{1}{8}\left(\frac{1}{K_c^2} - K_c^2\right). \end{aligned} \tag{22}$$

We stress that Eq. (20) is independent of σ and that the dependence on K_s is through the overall normalization constant Z_1 and the boundary reflection amplitude only. The one-particle contributions of the form-factor expansion are given by the first two terms in Eq. (20), while the dots represent corrections involving a higher number of particles in the intermediate state as well as higher-order corrections due to the boundary. We have determined the subleading terms in the spin part of the Green function at the LEP and found their contribution to the LDOS calculated later to be negligible (see Sec. IV C).

After analytic continuation to real times $\tau \to \mathrm{i}t$, the Green function, Eq. (18), exhibits a light cone effect. The first term in Eq. (20) shows oscillating behavior for $r^2 < (v_s t)^2$ but is damped otherwise. Similarly, the second term is oscillating for $4R^2 < (v_s t)^2$. These oscillations are due to the propagation of spinons from x_2 to x_1 either directly or via the boundary. In particular, at late enough times both terms will oscillate. A similar light cone effect was observed[48] in the Ising model with a boundary. On the other hand, the charge part, Eq. (19), possesses singularities at $v_c t = \pm r$ and $v_c t = \pm 2R$ due to the propagation of antiholons.

The low-momentum regime of the Fourier transform of the LDOS is obtained from ($\tau > 0$, $x_1 < x_2$)

$$\begin{aligned} G^{RR}_{\sigma\sigma'}(\tau,x_1,x_2) &= -\frac{\delta_{\sigma\sigma'}}{2\pi}\frac{1}{(v_c\tau - \mathrm{i}r)^a}\frac{1}{(v_c\tau + \mathrm{i}r)^b}\left[\frac{4x_1x_2}{(v_c\tau - 2\mathrm{i}R)(v_c\tau + 2\mathrm{i}R)}\right]^c \\ &\quad \times Z_1\left[\frac{1}{\pi}\sqrt{\frac{\mathrm{i}\tau - r/v_s}{\mathrm{i}\tau + r/v_s}}K_{1/2}\left(\Delta\sqrt{\tau^2 + r^2/v_s^2}\right) + \int_{-\infty}^{\infty}\frac{d\theta}{2\pi}K\left(\theta + \mathrm{i}\frac{\pi}{2}\right)e^{2\mathrm{i}\frac{\Delta}{v_s}R\sinh\theta}e^{-\Delta\tau\cosh\theta} + \cdots\right] \\ &= G^{LL}_{\sigma\sigma'}(\tau,x_2,x_1). \end{aligned} \tag{23}$$

Compared to G^{RL}, the singularity at $v_c t = 2R$ is much softer, whereas the one at $v_c t = r$ is more pronounced.

IV. LOCAL DENSITY OF STATES

The knowledge of the Green function, Eq. (16), enables us to calculate the LDOS, which is directly related to the tunneling current measured in STM experiments. As noted in Ref. 9 it is useful to consider the Fourier transform of the LDOS, as physical properties can be more easily identified. For example, this technique was used to study quasiparticle interference in high-temperature superconductors[3,4] and rare-earth compounds.[6] We first consider the boundary condition $\Psi_\sigma(0) = 0$, which results in the Green function, Eq. (18), and hence yields a spin-independent LDOS. More general boundary conditions may lead to a spin-dependent LDOS or even the formation of a boundary bound state. We discuss this case in the next section.

The Fourier transform of the LDOS is given by $N_\sigma(E,Q) = N^>_\sigma(E,Q) + N^<_\sigma(E,Q)$, where

$$\begin{aligned} N^>_\sigma(E,Q) = -\frac{1}{2\pi}\int_{-\infty}^{0}dx\int_{-\infty}^{\infty}dt\,e^{\mathrm{i}(Et - Qx)} \\ \times G_{\sigma\sigma}(\tau > 0,x,x)\Big|_{\tau\to\mathrm{i}t+\delta} \end{aligned} \tag{24}$$

$$\begin{aligned} N^<_\sigma(E,Q) = \frac{1}{2\pi}\int_{-\infty}^{0}dx\int_{-\infty}^{\infty}dt\,e^{\mathrm{i}(Et - Qx)} \\ \times G_{\sigma\sigma}(\tau < 0,x,x)\Big|_{\tau\to\mathrm{i}t-\delta} \end{aligned} \tag{25}$$

Here the Green function has been analytically continued to real times and we have take the limit $x_1 \to x_2 \equiv x$. We focus on the LDOS for positive energies in what follows but note that the LDOS for negative energies can be analyzed analogously. As already mentioned, we are mainly concerned with the $2k_F$ component, as it vanishes in the absence of the boundary and hence offers a particularly clean way of investigating boundary effects. For $Q \approx 2k_F$, only $G^{RL}_{\sigma\sigma}$ contributes, and starting from Eq. (18) we arrive at the following expression (see Appendix D):

$$N^>_\sigma(E,2k_F + q) = \sum_{i=1}^{2}N^>_i(E,2k_F + q) + \cdots, \tag{26}$$

$$\begin{aligned} N^>_i(E,2k_F + q) &= -\Theta(E - \Delta)\frac{Z_1\,e^{-\mathrm{i}\frac{\pi}{4}(4c+1)}\,\Gamma(2c+1)}{8\pi^2\,v_c^{a+b-1}\,\Gamma(a+b+2c)} \\ &\quad \times \int_{-A}^{A}d\theta\frac{h_i(\theta)\,u_i^{2c+1}}{(E - \Delta\cosh\theta)^{2-a-b}} \\ &\quad \times F_1(2c+1,a,b,a+b+2c;u_i^*,-u_i). \end{aligned} \tag{27}$$

Here $|q| \ll 2k_F$, $A = \operatorname{arcosh}(\frac{E}{\Delta})$, F_1 denotes Appell's hypergeometric function[49] (see Appendix E), $h_1(\theta) = 1, h_2(\theta) = K(\theta + i\frac{\pi}{2})\, e^{\theta/2}$, and

$$u_1 = \frac{2}{v_c q}(E - \Delta\cosh\theta) + i\,\mathrm{sgn}\left(\frac{v_s q}{\Delta}\right)\delta,$$
$$u_2 = \frac{2v_s}{v_c}\,\frac{E - \Delta\cosh\theta}{v_s q - 2\Delta\sinh\theta} + i\,\mathrm{sgn}\left(\frac{v_s q}{\Delta} - 2\sinh\theta\right)\delta, \tag{28}$$

where $\delta \to 0+$. The result, Eq. (27), is valid for $a + b < 2$ and $-1/2 < c$. Here we plot $N_\sigma^>(E, 2k_F + q)$ for two parameter regimes. We smear out singularities by taking δ small but finite ($\delta = 0.01$ unless stated), which mimics broadening by instrumental resolution and temperature in experiments. The results presented here apply to the regime $T \ll E, \Delta, v_c/a_0$ (a_0 is the lattice spacing), where temperature effects are negligible.

A. Repulsive case

We first consider the case $v_s < v_c$, $K_c < 1$. This can be thought of as providing a simplified model for the LDOS of a two-leg ladder with repulsive electron-electron interactions. The low-energy theory for the ladder is similar in that there is a gapless charge sector and a gapped spin sector, but the full description of the latter is considerably more complicated.[35]

In Figs. 1 and 2 we plot $N_\sigma^>(E, 2k_F + q)$ for the case of unbroken spin rotational symmetry ($K_s = 1$). The Fourier transform of the LDOS is dominated by a singularity at momentum $2k_F$ ($q = 0$), which arises from the contribution $N_1^>$. For fixed energy and close to singularity, this term behaves as (see Appendix F)

$$N_1^>(E, 2k_F + q) \sim \left(\frac{1}{v_c q}\right)^\alpha, \quad \alpha = 1 - \frac{K_c^2}{2}, \tag{29}$$

which implies a phase jump of $\pi\alpha$ as $q \to 0\pm$. This peak is indicative of the CDW order being pinned at the boundary. We note, however, that the peak occurs at finite energies and hence the underlying process is not static. A similar feature can be seen in the Luttinger liquid case,[9] where the singularity as a function of q is softer [$\alpha_{LL} = (1 - K_c^2)/2$].

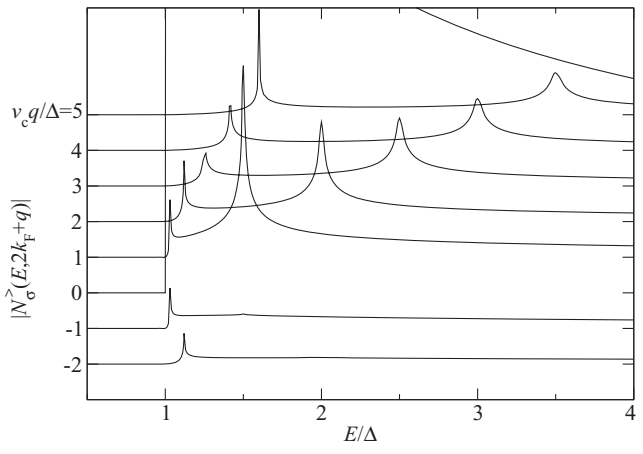

FIG. 1. $|N_\sigma^>(E, 2k_F + q)|$ (in arbitrary units) for $K_c = 0.8$, $K_s = 1$, and $v_c = 2v_s$. Curves are constant q scans that have been offset along the y axis by a constant with respect to one another. The LDOS is dominated by a strong peak at $q = 0$, i.e., $Q = 2k_F$. We further observe dispersing features at $E_c = v_c|q|/2 + \Delta$ and $E_s = \sqrt{(v_s q/2)^2 + \Delta^2}$. For $q < 0$ the dispersing features are strongly suppressed.

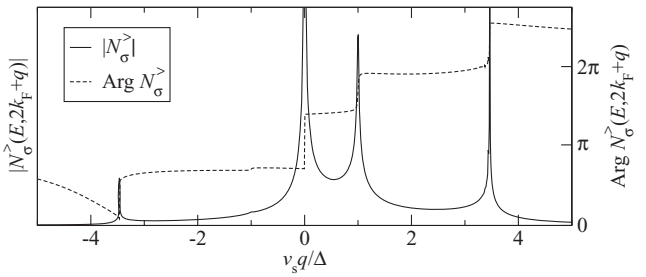

FIG. 2. Constant energy scan for $E = 2\Delta$: $|N_\sigma^>(E, 2k_F + q)|$ (in arbitrary units) and $\mathrm{Arg} N_\sigma^>(E, 2k_F + q)$ for $K_c = 0.8$, $K_s = 1$, and $v_c = 2v_s$. We observe a peak at $q = 0$ (related to the pinning of the CDW at the boundary) and dispersing features at $q = \pm 2(E - \Delta)/v_c$ as well as $q = \pm 2\sqrt{E^2 - \Delta^2}/v_s$. For $q < 0$ the dispersing features are strongly suppressed. Furthermore, we observe characteristic jumps in the argument at the positions of the peaks.

At low energies above the spin gap Δ we further observe two dispersing features, associated with the collective spin and charge degrees of freedom, respectively. These are broadly similar to the *bulk* single-particle spectral function[50,51] and feature (1) a "charge peak" that follows

$$E_c(q) = \frac{v_c|q|}{2} + \Delta \tag{30}$$

and (2) a "spin peak" at position

$$E_s(q) = \sqrt{\left(\frac{v_s q}{2}\right)^2 + \Delta^2}. \tag{31}$$

We note that neither peak is sharp (i.e., they are not δ-functions) and hence have to be thought of as arising from excitations involving at least two "elementary" constituents. In this way of thinking, the charge peak arises from two-particle excitations composed of a "zero-momentum" spinon contributing an energy Δ and a gapless antiholon of "momentum" q. On the other hand, the spin peak can be thought of arising from two-particle excitations composed of a "zero-momentum" antiholon and a spinon of "momentum" q. The appearance of $v_c/2$ and $v_s/2$ in Eqs. (30) and (31), respectively, is due to the fact that the particles have to propagate to the boundary and back, thus covering the distance $2x$ in time t. We note that on a technical level the charge peak arises from the contribution $N_1^>$ to the Fourier transform of the LDOS, whereas the spin peak has its origin in $N_2^>$, which encodes the effects of the boundary on the spin degrees of freedom. In the $q < 0$ region the dispersing features are strongly suppressed, and for $K_c = 1$ the charge feature is found to vanish entirely.

It is instructive to plot $N_\sigma^>(E, 2k_F + q)$ as a function of q for fixed energy; see Fig. 2. We observe characteristic jumps in the phase $\mathrm{Arg}\, N_\sigma^>$ at the peak positions. This is similar to the Luttinger liquid case.[9]

B. Attractive case

We now turn to the case of a CDW state arising in a system with (effective) attractive electron-electron interactions. As

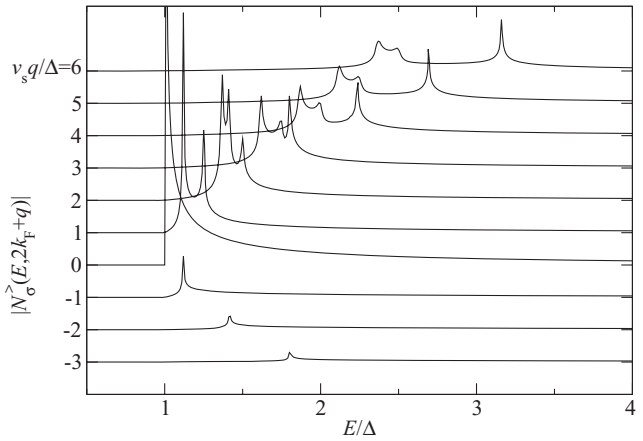

FIG. 3. $|N_\sigma^>(E,2k_\mathrm{F}+q)|$ (in arbitrary units) for $K_\mathrm{c}=1.2$, $K_\mathrm{s}=1$, and $v_\mathrm{s}=2v_\mathrm{c}$. Curves are constant q scans that have been offset along the y axis by a constant with respect to one another. The peak at $q=0$ is much less pronounced then in the repulsive case (see Fig. 1). We observe dispersing features at E_c, E_s, and $E_\mathrm{cs}=v_\mathrm{c}|q|/2+\Delta\sqrt{1-(v_\mathrm{c}/v_\mathrm{s})^2}$ (for $|q|>q_0$ only).

discussed in Sec. II, this case arises in electron-phonon systems. The effective parameters are given by $v_\mathrm{s}>v_\mathrm{c}$ and $K_\mathrm{c}>1>K_\mathrm{s}$.

In Fig. 3 we plot $N_\sigma^>(E,2k_\mathrm{F}+q)$ as a function of energy for several values of q (in units of the spin gap). We again observe a singularity at $2k_\mathrm{F}$, which arises from Eq. (29). The singularity is much less pronounced than in the repulsive case and disappears for $K_\mathrm{c}\geqslant\sqrt{2}$. As in the repulsive case there are several dispersing features:

(1) A charge peak at $E=E_\mathrm{c}(q)$, where E_c is given by Eq. (30).

(2) A spin peak at $E=E_\mathrm{s}(q)$, where E_s is defined in Eq. (31).

(3) When $|q|$ exceeds a critical value q_0, a third dispersing low-energy peak that appears (see Fig. 4) at

$$\begin{aligned} E_\mathrm{cs}(q) &= \frac{v_\mathrm{c}|q|}{2}+\Delta\sqrt{1-\left(\frac{v_\mathrm{c}}{v_\mathrm{s}}\right)^2} \\ &= E_\mathrm{s}(q_0)+\frac{v_\mathrm{c}}{2}(|q|-q_0), \qquad (32) \\ q_0 &= \frac{2\Delta v_\mathrm{c}}{v_\mathrm{s}\sqrt{v_\mathrm{s}^2-v_\mathrm{c}^2}}. \end{aligned}$$

This feature can be thought of as arising from a "momentum" q_0 spinon and an antiholon carrying "momentum" $q-q_0$. We note that in this case the spin and charge excitations have the same group velocity:

$$\frac{\partial E_\mathrm{c}}{\partial q}=\left.\frac{\partial E_\mathrm{s}}{\partial q}\right|_{q=q_0}=\frac{v_\mathrm{c}}{2}. \qquad (33)$$

This behavior is reminiscent of what is found for the single-particle spectral function in the bulk.[50,51] The peak splitting, and hence the qualitative difference between the repulsive and the attractive regime, is a consequence of the curvature of the (anti-)soliton dispersion relation and hence of the spin gap. In the Luttinger liquid case[9] (where both sectors are massless), there are only two dispersing features in both regimes.

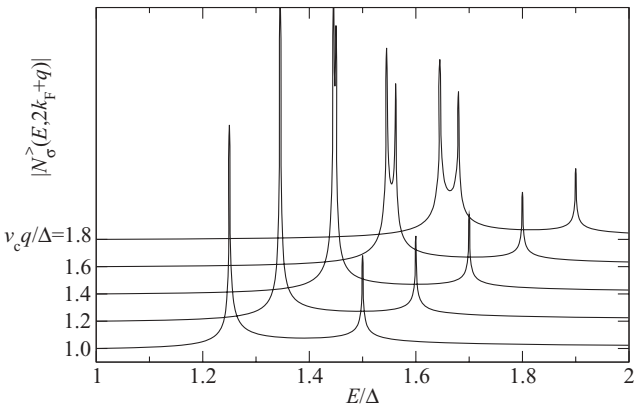

FIG. 4. $|N_\sigma^>(E,2k_\mathrm{F}+q)|$ (in arbitrary units) for $K_\mathrm{c}=1$, $K_\mathrm{s}=1/\sqrt{2}$, $v_\mathrm{s}=1.5\,v_\mathrm{c}$, $\delta=0.001$, and $v_\mathrm{c}q/\Delta=1.0,\ldots,1.8$. Curves have been offset along the y axis by a constant with respect to one another. We observe the splitting of the spin peak at E_s at the critical momentum $v_\mathrm{c}q_0/\Delta\approx1.19$.

C. Higher-order corrections

As we have indicated in Eq. (20) there are contributions to the LDOS beyond those already discussed. They arise from our calculation of the spin part of the Green function and are expected to be small.[48] To verify that they can indeed be neglected, we have analyzed them in some detail at the LEP $K_\mathrm{s}=1/\sqrt{2}$, where the necessary matrix elements take a particularly simple form, which makes the actual calculations much easier.

Our purpose is then to determine further terms in the the expansion, Eq. (26), of $N_\sigma^>(E,2k_\mathrm{F}+q)$. We denote by N_{nm} the contribution to Eq. (26) that arises from processes in which n gapped spinons (which correspond to solitons or antisolitons in the sine-Gordon model describing the spin sector) propagate between $(0,x_2)$ and (τ,x_1), and that involves the mth power of the boundary reflection matrix K. The foregoing terms correspond to $N_{10}=N_1^>$ and $N_{01}=N_2^>$. In Appendix C4 we present some details of the calculation of the terms in the form-factor expansion of $g_s(\tau,x_1,x_2)$ that give rise to N_{nm} with $m+n\leqslant3$. The number of θ integrations in N_{nm} equals $m+n$ [cf. Eq. (27)]. We find that their contributions to the Fourier transform of the LDOS are small. In particular, all qualitative features of the LDOS such as dispersing peaks are already encoded in N_{10} and N_{01}. In Fig. 5 we show the leading terms N_{10} and N_{01} as well as the subleading terms for $K_\mathrm{c}=1$ and $v_\mathrm{c}>v_\mathrm{s}$ for a fixed value of q as a function of energy. We see that the two leading terms in Eq. (26) indeed capture all qualitative features of the LDOS and carry the main part of the spectral weight at low energies $E\leqslant5\Delta$. The higher-order terms are small compared to N_{10} and N_{01}. In particular, N_{30} vanishes for $E<3\Delta$, since this term originates from a three-particle process. In general, all terms N_{nm} originating from n-particle processes vanish for $E<n\Delta$. Most importantly, however, the higher-order terms do not possess any singularities. The suppression of subleading terms in the form-factor expansion for bulk two-point functions is a well-known feature of massive theories,[44,52,53] whereas the smallness of terms involving higher powers of the boundary

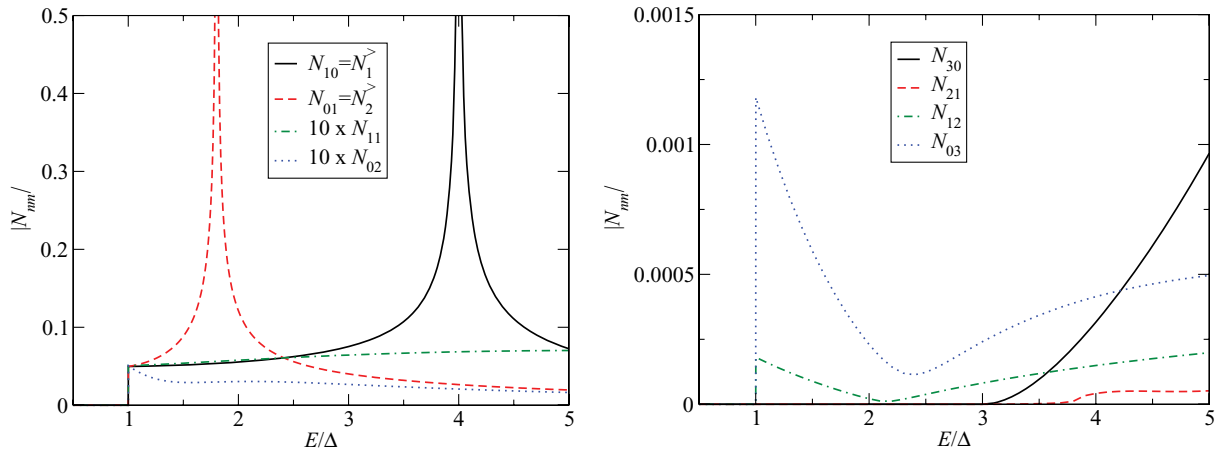

FIG. 5. (Color online) Left: Comparison of the absolute values of $N_{10} = N_1^>(E,2k_F + q)$ and $N_{01} = N_2^>(E,2k_F + q)$ to the subleading terms N_{11} and N_{02} ($N_{20} = 0$). We stress that the scale for the higher-order terms has been magnified. Right: Absolute values of the terms N_{30}, N_{21}, N_{12}, and N_{03}. We stress the different scales on the y axis. Parameters are $K_c = 1$, $K_s = 1/\sqrt{2}$, $v_c = 2v_s$, and $v_s q/\Delta = 3$. The three-particle contributions N_{30} and N_{21} vanish for $E < 3\Delta$. Furthermore, the higher-order terms possess no peaks.

reflection amplitude K has recently been demonstrated for the Ising model with a boundary magnetic field.[48]

D. Low-momentum regime

The low-momentum regime $Q \approx 0$ of the Fourier transform of the LDOS can be analyzed in the same way as in the $Q \approx 2k_F$ case already discussed. We note that the LDOS for $Q \approx 0$ is nonvanishing even in the absence of a boundary.[50,51] In the presence of a boundary the Fourier transform of the LDOS for $Q \approx 0$ is obtained from Eq. (23). The leading terms are given by $N_\sigma^>(E,Q) = \sum_{i=1}^2 N_i^>(E,Q) + \ldots$, where

$$N_i^>(E,Q) = -\Theta(E-\Delta)\,\frac{Z_1\, e^{-i\frac{\pi}{2}(2c+1)}\,\Gamma(a+b+1)}{4\pi^2\, v_c^{a+b-1}\,\Gamma(2a+2b)} \times \int_{-A}^{A} d\theta \frac{h_i(\theta)\, u_i^{2c+1}}{(E-\Delta\cosh\theta)^{2-a-b}} \times F_1(a+b+1,c,c,2a+2b;u_i^*,-u_i). \quad (34)$$

Here we have $|Q| \ll k_F$, $A = \operatorname{arcosh}(\frac{E}{\Delta})$, $h_1(\theta) = e^{\theta/2}$, and $h_2(\theta) = K(\theta + i\frac{\pi}{2})$, and $u_{1,2}$ are defined in Eq. (28), with q replaced by Q. The main difference from Eq. (26) is in the dependence of Appell's hypergeometric function on K_c.

In Figs. 6 and 7 we plot $N_\sigma^>(E,Q)$ for the case of repulsive electron interactions and unbroken spin rotational symmetry. It is dominated by a singularity at $Q = 0$, which has its origin in $N_1^>$ and behaves as $\sim 1/Q$ independently of K_c. This singularity is more pronounced than its counterpart at $2k_F$. We further observe dispersing features at positions $E_c(Q)$ and $E_s(Q)$, respectively. Both of these are symmetric under $Q \to -Q$. The peak at $E_c(Q)$ is strongly suppressed, vanishes for $K_c = 1$, and becomes a dip in the attractive regime. The suppression is due to the softness of the singularities of G^{RR} at $v_c t = 2R$. In contrast, the charge part of Eq. (23) has its strongest singularity at $v_c t = r = 0$, which results in a background of spectral weight in $N_\sigma^>(E,Q)$ for all energies above the spin gap.

In the attractive case ($v_s > v_c$) we observe a peak splitting similar to that in the $2k_F$ component, but all peaks are very weak.

V. GENERAL BOUNDARY CONDITIONS AND BOUNDARY BOUND STATES

So far we have considered the simplest possible boundary conditions corresponding to a spin-independent phase shift of π. Both ways of realizing a boundary in a (quasi-) 1D system that we have discussed (i.e. as a result of an impurity or in a "two-tip" STS experiment) are expected to give rise to a local potential or magnetic field. These correspond to more general phase shifts for reflection of particles at the boundary. As is well known, such more general boundary conditions can give rise to boundary bound states (see, e.g., Ref. 54). These are expected to be visible in the Fourier transform of the LDOS as

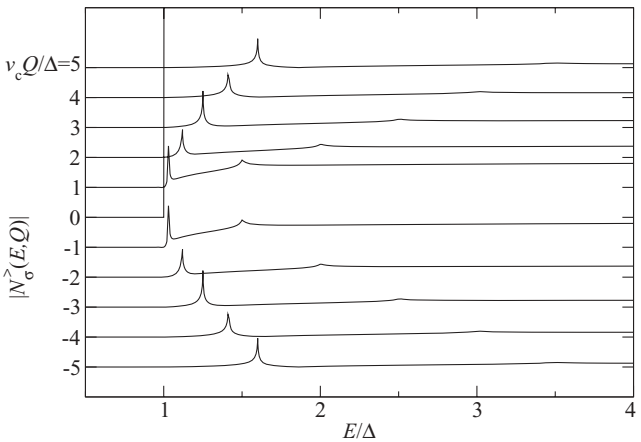

FIG. 6. $|N_\sigma^>(E,Q)|$ (in arbitrary units) for $K_c = 0.8$, $K_s = 1$, and $v_c = 2v_s$. Curves are constant Q scans that have been offset along the y axis by a constant with respect to one another. We observe dispersing features at $E_c(Q)$ and $E_s(Q)$. Charge features are very weak for all momenta. We further observe a constant background at energies higher than the spin gap.

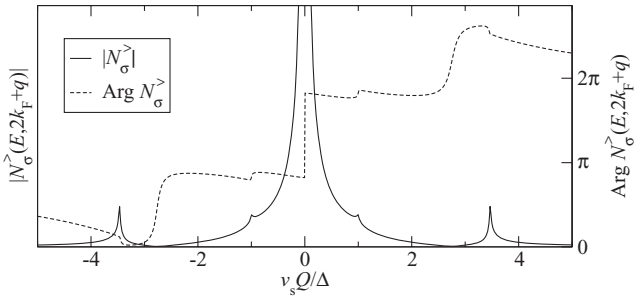

FIG. 7. Constant energy scan for $E = 2\Delta$: $|N_\sigma^>(E,Q)|$ (in arbitrary units) and $\mathrm{Arg}N_\sigma^>(E,Q)$ for $K_c = 0.8$, $K_s = 1$, and $v_c = 2v_s$. We observe a strong peak at $Q = 0$ and dispersing features at $Q = \pm 2(E-\Delta)/v_c$ as well as $Q = \pm 2\sqrt{E^2-\Delta^2}/v_s$. Note that $|N_\sigma^>(E,Q)|$ is symmetric under $Q \to -Q$.

"resonances" inside the single-particle gap. This is most easily seen by considering a Lehmann representation of $N_\sigma^>(E,Q)$ in terms of the eigenstates $|n_b\rangle$ on the half-line:

$$N_\sigma^>(E,Q) = \int_{-\infty}^{0} dx\, e^{-iQx} \sum_{n_b} |\langle 0_b|\Psi_\sigma(0,x)|n_b\rangle|^2 \delta(E - E_{n_b}). \tag{35}$$

For boundary bound states $|\mathrm{bbs},\alpha\rangle$ we have $0 < E_{\mathrm{bbs},\alpha} < \Delta$, which leads to features in $N_\sigma^>(E,Q)$ below the single-particle gap. Because we are dealing with a spin-charge separated system, these features will generally not be sharp, as the bound state occurs only in the gapped sector of the theory. We now turn to calculating the LDOS in cases where boundary bound states exist. We first consider boundary conditions of the form

$$R_\sigma(\tau,0) = -e^{-if_\sigma \Phi_s^0/2} L_\sigma(\tau,0), \tag{36}$$

where $f_\uparrow = 1 = -f_\downarrow$. In terms of the Bose fields these boundary conditions read

$$\Phi_c(\tau,0) = 0, \quad \Phi_s(\tau,0) = \Phi_s^0, \quad 0 \leqslant \Phi_s^0 < \pi. \tag{37}$$

We note that these boundary conditions break spin rotational symmetry. However, if we go over to the case of a 1D Mott insulator by exchanging spin and charge degrees of freedom, the spin rotational symmetry remains intact and the boundary conditions correspond to a local potential.

As before, we focus on the $2k_F$ component of the Fourier transform of the LDOS. As we have changed the boundary conditions only in the spin sector, the charge part, Eq. (19), of the chiral Green function remains unchanged.

The two leading terms of the form-factor expansion in the spin sector are still of the form, Eq. (20), but now the boundary reflection amplitude K is different and, in particular, is spin dependent. At the LEP it is given by[45]

$$K^{\sigma\bar\sigma}(\theta) = \frac{\sin\left(i\frac{\theta}{2} - f_\sigma \frac{\Phi_s^0}{2}\right)}{\cos\left(i\frac{\theta}{2} + f_\sigma \frac{\Phi_s^0}{2}\right)}, \qquad K^{\sigma\sigma}(\theta) = K^{\bar\sigma\bar\sigma}(\theta) = 0. \tag{38}$$

Here we have introduced the notations $\uparrow = +$ and $\downarrow = -$ as well as $\bar\sigma = -$ for $\sigma = +$ and vice versa. We note that as a result of the different choice of phase for the asymptotic states, Eq. (38) differs by a minus sign from Ref. 45 (see also Appendix C). The expressions for general K_s are given in Refs. 29, 46, and 47.

In the spin rotationally symmetric case $K_s = 1$ we have $K^{+-}(\theta) = K^{-+}(\theta) = K(\theta)$, where $K(\theta)$ is given in Eq. (21). We stress that the Green function remains diagonal in spin space, $G^{RL}_{\sigma\sigma'} \propto \delta_{\sigma\sigma'}$, and that the spin dependence is entirely due to the boundary reflection matrix $K^{\sigma\bar\sigma}$. Before presenting the resulting LDOS we discuss the emergence of a boundary bound state in the spin sector.[29,46,55] If we choose the phase shift Φ_s^0 in the spin sector such that

$$K_s^2 \pi < \Phi_s^0, \tag{39}$$

the boundary reflection amplitude $K^{-+}(\theta)$ has a pole in the physical strip $0 \leqslant \Im\mathrm{m}\,\theta \leqslant \pi/2$. This pole corresponds to a boundary bound state with energy

$$E_{\mathrm{bbs}} = \Delta \sin\gamma, \quad \gamma = \frac{\pi - \Phi_s^0}{2 - 2K_s^2}. \tag{40}$$

The physical nature of the bound state has been discussed by Ghoshal and Zamolodchikov.[29] The classical ground state of the sine-Gordon model on the half-line, Eq. (14), in the entire range $0 \leqslant \Phi_s^0 < \pi$ is characterized by the asymptotic behavior $\Phi_s \to 0$ as $x \to -\infty$. In contrast, there exists a second classically stable state satisfying $\Phi_s \to 2\pi$ as $x \to -\infty$. When Φ_s^0 is sufficiently large this state is expected to be stable in the quantum theory as well.

We note that for $\Phi_s^0 = \pi$ both states are degenerate and Eq. (40) vanishes. In the attractive regime of the sine-Gordon model $K_s < 1/\sqrt{2}$ additional boundary bound states occur, while in the spin rotationally invariant case $K_s \to 1$ the condition $K_s^2\pi < \Phi_s^0 < \pi$ is never satisfied and hence no boundary bound states exist.

When calculating dynamical response functions in the boundary-state formalism, additional contributions in the form-factor expansions occur upon analytical continuation in the rapidity variables. In particular, the pole of the boundary reflection amplitude in the physical strip gives rise to an additional term linear in K in the form-factor expansion, Eq. (20). In the case $\tau > 0$ and $x_1 < x_2$ it takes the form (see Appendix C 5)

$$\Theta\left(\Phi_s^0 - K_s^2\pi\right) \delta_{\sigma\downarrow}\, Z_1\, B\, e^{i\frac{\gamma}{2}}\, e^{2\frac{\Delta}{v_s} R\cos\gamma}\, e^{-\Delta\tau\sin\gamma}, \tag{41}$$

where the constant $B \geqslant 0$ is related to the residue of $K^{\mp\pm}(\theta)$ [see Eq. (C47)]. At the LEP $B = -2\cos\Phi_s^0$. We stress that this additional term appears in the down-spin channel only, since we have assumed $0 \leqslant \Phi_s^0 < \pi$. If we were to consider $-\pi < \Phi_s^0 \leqslant 0$, we would find a term similar to Eq. (41) in the up-spin channel only.

The Fourier transform of the LDOS for the boundary conditions, Eq. (37), can be expanded as before and is expressed as

$$N_\sigma^>(E,2k_F+q) = \sum_{i=1}^{3} N_{\sigma,i}^>(E,2k_F+q) + \cdots. \tag{42}$$

Here the first two terms are again of the form, Eq. (27), where in the second term, $N_{\sigma,2}^>$, we need to replace the boundary

reflection amplitude $K(\theta+\mathrm{i}\frac{\pi}{2})$ by its spin-dependent counterpart $K^{\sigma\bar{\sigma}}(\theta+\mathrm{i}\frac{\pi}{2})$. The third term is obtained from Eq. (41) and arises as a result of the presence of a boundary bound state. Explicitly it reads

$$N^{>}_{\sigma,3}(E,2k_{\mathrm{F}}+q)=\Theta\big(\Phi^0_{\mathrm{s}}-K^2_{\mathrm{s}}\,\pi\big)\,\Theta(E-E_{\mathrm{bbs}})\,\delta_{\sigma\downarrow}\,\frac{Z_1 B}{4\pi}\,\frac{\Gamma(2c+1)}{\Gamma(a+b+2c)}\,\frac{\mathrm{i}\,e^{\frac{\mathrm{i}}{2}\gamma}\,e^{-\mathrm{i}\pi c}}{v_{\mathrm{c}}^{a+b-1}}$$
$$\times\,\frac{\big(\frac{2}{v_{\mathrm{c}}q}(E-E_{\mathrm{bbs}})+\mathrm{i}\,\mathrm{sgn}\big(\frac{v_{\mathrm{s}}q}{\Delta}\big)\,\delta\big)^{2c+1}}{(E-E_{\mathrm{bbs}})^{2-a-b}}\,F^{(3)}_{\mathrm{D}}(2c+1,a,b,2c,a+b+2c;u^*_3,-u_3,-u'_3). \tag{43}$$

Here $F^{(3)}_{\mathrm{D}}$ denotes Lauricella's hypergeometric function of three arguments[56] (see Appendix E), and

$$u_3=\frac{2}{v_{\mathrm{c}}q}(E-E_{\mathrm{bbs}})+\mathrm{i}\frac{2\Delta}{v_{\mathrm{s}}q}\cos\gamma,\quad u'_3=\mathrm{i}\frac{2\Delta}{v_{\mathrm{s}}q}\cos\gamma, \tag{44}$$

where the constant γ is defined in Eq. (40). The Fourier transform of the LDOS, Eq. (42), has a nondispersing singularity at its lower threshold:

$$N^{>}_{\sigma,3}(E,2k_{\mathrm{F}}+q)\propto\frac{\delta_{\sigma\downarrow}}{(E-E_{\mathrm{bbs}})^{\alpha}},\quad \alpha=1-\frac{1}{2K^2_{\mathrm{c}}}. \tag{45}$$

The emergence of a nondispersing feature within the spin gap signals the presence of a boundary bound state. In Fourier space the LDOS is a convolution of contributions from the spin and charge sectors. As we are dealing with a bound state in the spin sector, the exponent of the singularity depends only on the Luttinger parameter in the charge sector. We note that the singularity occurs only in the down-spin channel and disappears for $K^2_{\mathrm{c}}\leqslant 1/2$. In contrast, in $N^{<}_{\sigma}$ the additional feature due to the boundary bound state appears only in the up-spin channel.

In Fig. 8 we plot the down-spin component of Eq. (42) for $v_{\mathrm{c}}>v_{\mathrm{s}}$ as a function of energy for several values of q. As before, at low energies above the spin gap Δ we observe two dispersing features associated with the collective spin and charge degrees of freedom that follow E_{s} and E_{c}, respectively. In addition, we observe the nondispersing singularity, Eq. (45), at $E=E_{\mathrm{bbs}}$.

In Fig. 9 we plot $N^{>}_{\uparrow}$ and $N^{>}_{\downarrow}$ as functions of energy for $v_{\mathrm{c}}<v_{\mathrm{s}}$. We see that the singularity arising due to the presence of a boundary bound state appears only in the down-spin channel. For either spin polarization we observe three dispersing features, at $E_{\mathrm{c}}(q)$, $E_{\mathrm{s}}(q)$, and $E_{\mathrm{cs}}(q)$, respectively. Their interpretations are completely analogous to the discussion in Sec. IV B. In addition to these sharp peaks, we observe a broad maximum in the down-spin channel at energies $E\approx E_{\mathrm{bbs}}+v_{\mathrm{c}}q/2$. This feature is suppressed for $v_{\mathrm{c}}>v_{\mathrm{s}}$; see Fig. 8. Its physical origin is the simultaneous excitation of the boundary bound state and a finite-energy excitation in the charge sector. We note that the asymmetry in $N^{>}_{\uparrow}(E,Q)-N^{>}_{\downarrow}(E,Q)$ could, in principle, be detected in experiments using a magnetic STM tip. So far we have considered only hard-wall boundary conditions in the charge sector, that is, $\Phi_{\mathrm{c}}(x=0)=0$. Our analysis can be straightforwardly extended to the case $\Phi_{\mathrm{c}}(x=0)=\Phi^0_{\mathrm{c}}$, which, in terms of the original electrons, corresponds to a local potential close to the boundary.

VI. FINITE-TEMPERATURE LDOS

Another interesting issue concerns the effects of a finite temperature on the LDOS. The regime $T\lesssim\Delta/2$ can, in principle, be analyzed by generalizing the methods recently developed in Refs. 57 to the boundary state formalism. However, to keep matters simple we restrict ourselves to the regime of very low temperatures $T\ll\Delta$. Here the main effects arise from a modification of the dynamical response in the gapless charge sector and correlation functions in the spin sector can be approximated by their $T=0$ expressions. This is the case because we consider only response functions that involve both sectors. The charge part of the Green function $G^{RL}_{\sigma\sigma'}(\tau,x_1,x_2)=g_{\mathrm{c}}(\tau,x_1,x_2)\,g_{\mathrm{s}}(\tau,x_1,x_2)$ can be evaluated using conformal field theory methods[38,58] and is found to be

$$g_{\mathrm{c}}(\tau,x_1,x_2)=-\frac{\delta_{\sigma\sigma'}}{2\pi}\left(\frac{\pi}{v_{\mathrm{c}}\beta}\right)^{a+b}\frac{1}{\sin^a\big(\frac{\pi}{v_{\mathrm{c}}\beta}(v_{\mathrm{c}}\tau-2\mathrm{i}R)\big)}$$
$$\times\,\frac{1}{\sin^b\big(\frac{\pi}{v_{\mathrm{c}}\beta}(v_{\mathrm{c}}\tau+2\mathrm{i}R)\big)}$$
$$\times\left[\frac{\sinh\big(\frac{2\pi}{v_{\mathrm{c}}\beta}x_1\big)\,\sinh\big(\frac{2\pi}{v_{\mathrm{c}}\beta}x_2\big)}{\sin\big(\frac{\pi}{v_{\mathrm{c}}\beta}(v_{\mathrm{c}}\tau-\mathrm{i}r)\big)\,\sin\big(\frac{\pi}{v_{\mathrm{c}}\beta}(v_{\mathrm{c}}\tau+\mathrm{i}r)\big)}\right]^c. \tag{46}$$

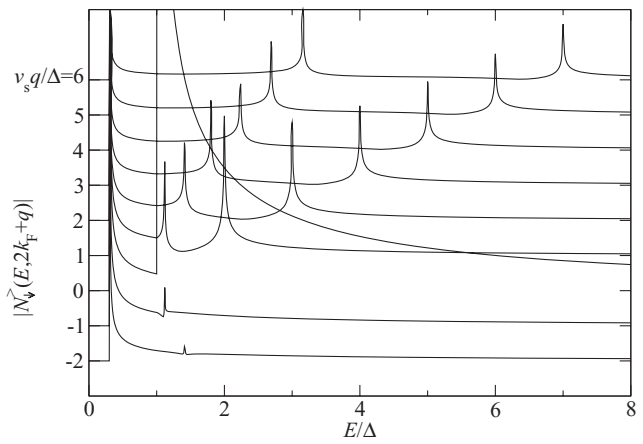

FIG. 8. $|N^{>}_{\downarrow}(E,2k_{\mathrm{F}}+q)|$ (in arbitrary units) for $K_{\mathrm{c}}=1$, $K_{\mathrm{s}}=1/\sqrt{2}$, $v_{\mathrm{c}}=2v_{\mathrm{s}}$, and $\Phi^0_{\mathrm{s}}=0.9\pi$. Curves are constant q scans that have been offset along the y axis by a constant with respect to one another. We observe dispersing features at $E_{\mathrm{s}}(q)$ and $E_{\mathrm{c}}(q)$ (for $q>0$ only) as well as a nondispersing singularity at $E=E_{\mathrm{bbs}}$, which is due to the formation of a boundary bound state in the spin sector.

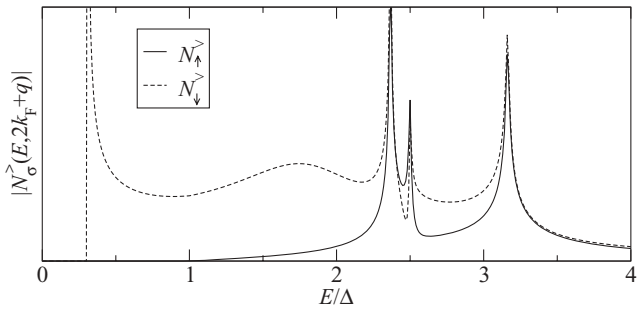

FIG. 9. $|N^>_\uparrow(E,2k_F+q)|$ (solid line) and $|N^>_\downarrow(E,2k_F+q)|$ (dashed line) for $v_s q/\Delta = 6$, $K_c = 1$, $K_s = 1/\sqrt{2}$, $v_s = 2v_c$, and $\Phi^0_s = 0.9\pi$. The broad maximum at $E \approx 1.8$ is caused by the excitation of the boundary bound state and additional charge excitations.

Here $\beta = 1/k_B T$ and the exponents in the charge sector are defined in Eq. (22). As we have already discussed, the spin part $g_s(\tau,x_1,x_2)$ is given by Eq. (20).

The particle contribution to the Fourier transform of the LDOS is still given by Eq. (24). The form-factor expansion in the spin sector results in the series expansion $N^>_\sigma(E,2k_F+q) = \sum_i N^>_i(E,2k_F+q)$, where the first two terms can be cast in the form

$$N^>_i(E,2k_F+q) = \frac{Z_1\,\pi^{a+b}}{32\pi^5 v_c}\,\frac{e^{i\frac{\pi}{4}}\,e^{-i\frac{\pi}{2}(a+b+2c)}}{(v_c\beta)^{a+b-2}} \times \int_{-\infty}^{\infty} d\theta\, h_i(\theta) \int_{-\infty}^{\infty} dx \int_{-\infty}^{x} dy \times \frac{e^{\frac{i\beta}{2\pi}\left(E_i+\frac{v_c q_i}{2}\right)x}}{\sinh^a(x-i\delta)}\,\frac{e^{\frac{i\beta}{2\pi}\left(E_i-\frac{v_c q_i}{2}\right)y}}{\sinh^b(y-i\delta)} \times \left(\frac{\sinh\left(\frac{1}{2}(y-x)\right)}{\sinh\left(\frac{1}{2}(x+y-i\delta)\right)}\right)^{2c}, \quad (47)$$

$$h_1(\theta) = 1, \quad h_2(\theta) = K^{\sigma\bar{\sigma}}\left(\theta + i\tfrac{\pi}{2}\right) e^{\theta/2},$$
$$E_1 = E_2 = E - \Delta\cosh\theta,$$
$$q_1 = q, \quad q_2 = q - \frac{2\Delta}{v_s}\sinh\theta.$$

We have plotted $N^>_\sigma(E,2k_F+q)$ for different temperatures in Figs. 10–12. As expected a finite temperature leads to a softening of the spectral gap Δ, a suppression of the peak related to the pinned CDW, and a broadening of the dispersing peaks. We observe that the effect of an increasing temperature on the spin peak is much stronger than the effect on the charge peak. The physical reason for this is as follows: in the CDW state, only the spin sector is protected by the gap. Thus for $T \ll \Delta$ there exists a significant number of antiholons in the thermal ground state. They will participate in the distribution of the external momentum q after the creation of an additional antiholon-spinon pair, thus leading to a decreased probability for the spinon to take the momentum q and thus to a suppression of the spin peak following $E_s(q)$. In contrast, the charge peak is not affected, as the antiholons possess a linear dispersion. This behavior is reminiscent of what is found for the bulk spectral functions.[51]

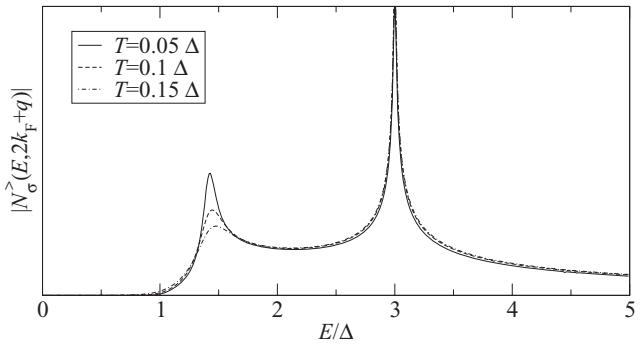

FIG. 10. $|N^>_\sigma(E,2k_F+q)|$ (in arbitrary units) for $v_s q/\Delta = 2$, $K_c = K_s = 1$, and $v_c = 2v_s$. We observe spectral weight within the spin gap and a broadening of the propagating peaks, which is much stronger for the spin peak at $E_s = \sqrt{(\frac{v_s q}{2})^2 + \Delta^2}$.

VII. IMPLICATIONS FOR STM EXPERIMENTS

STM experiments measure the local tunneling current, which is related to the LDOS by Eq. (1). In particular, the voltage dependence of the tunneling conductance measures the thermally smeared LDOS of the sample at the position of the tip. A possible spin dependence in the LDOS can be detected using a magnetic tip. As we have considered a 1D model, our results apply to quasi-1D materials at energies above the 1D-3D crossover scale, which is set by the strength of the 3D couplings. Furthermore, the main feature of the model we have studied is the existence of a spectral gap in one of the sectors, while the excitations in the other sector remain gapless. This situation is experimentally realized in various materials, for example, in two-leg ladder materials,[17] stripe phases of HTSCs,[5,9] carbon nanotubes,[1,16] Bechgaard salts,[14] and chain materials[15] like $SrCuO_2$ and Sr_2CuO_3. As our results show, STM experiments can be used to extract rather detailed information regarding bulk excitations by analyzing the modification of the LDOS due to a boundary or impurity.

Perhaps the most interesting materials to which our findings may be applied on a qualitative level are two-leg ladders like[59] $Sr_{14}Cu_{24}O_{41}$, which possesses a spin gap[60] of $\Delta \approx 550K$. The model we have studied captures the most basic features of the low-energy description of (weakly doped) two-leg ladders, namely, a gapless charge sector and a gapped spin sector. While the description of the spin sector for weakly doped two-leg ladders is considerably more involved, we expect the

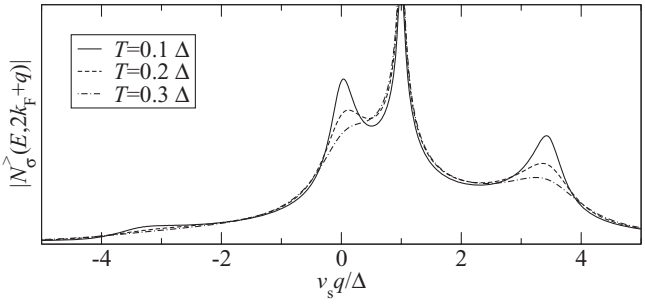

FIG. 11. Constant energy scan of $|N^>_\sigma(E,2k_F+q)|$ (in arbitrary units) for $E = 2\Delta$, $K_c = K_s = 1$, and $v_c = 2v_s$. We observe a suppression of the peak at $q = 0$ related to the pinned CDW.

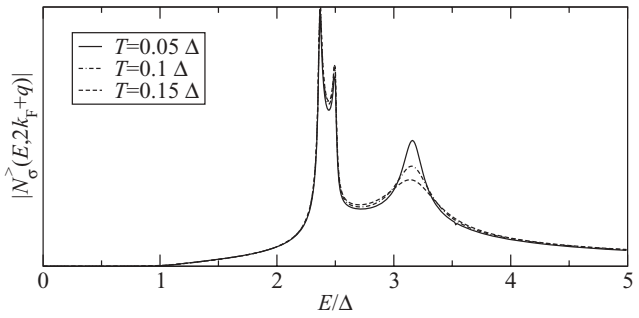

FIG. 12. $|N_\sigma^>(E,2k_F+q)|$ (in arbitrary units) for $v_s q/\Delta = 6$, $K_c = K_s = 1$, and $v_s = 2v_c$. We observe again that the broadening of the propagating spin peak is stronger than that of the other peaks.

gross features to be similar. In particular, we expect peaks to appear in $N_\sigma(E,Q)$, which correspond to the pinned CDW order, dispersing spin and charge degrees of freedom, and possibly boundary bound states. We note that our results apply to the regime $T \ll E, \Delta, v_c/a_0$, where temperature effects are negligible.

In Ref. 9 it was proposed that STM and STS experiments in HTSC can be used to detect "fluctuating stripes" (i.e., incommensurate spin and charge fluctuations on energy scales small compared to the superconducting gap) by rendering them static by the effects of impurities with a potential comparable to the (low) energy scales of these fluctuations. In that work it was also argued that 1D Luttinger liquids are effectively quantum critical systems and that a form of local (power law) CDW order is effectively induced by impurities (and edges) that pin the phase of the CDW, an effect that we have shown here to take place in a 1D Luther-Emery liquid associated with a CDW. STM and STS experiments in $Bi_2Sr_2CaCu_2O_{8+\delta}$ have confirmed the existence of both nondispersive spectral features in the LDOS associated with "fluctuating stripe order" as well as dispersive features associated with the propagating quasiparticles of the superconductor.[2,4,9] Recent STS experiments in $Bi_2Sr_2CaCu_2O_{8+\delta}$ have shown that the dispersive features of the LDOS disappear above the T_c of the superconductor, while the nondispersive features survive up to the temperature T^* at which the pseudogap closes.[61]

VIII. CONCLUSIONS

In this work we have determined the spatial Fourier transform of the LDOS of 1D CDW states and Mott insulators in the presence of a boundary. The latter may either model a strong potential impurity or be realized in a two-tip STM experiment. We found that the Fourier transform of the LDOS is dominated by a singularity at an energy equal to the single-particle gap Δ and at momentum $2k_F$. This feature is indicative of the pinning of the CDW order at the position of the impurity. We observed clear signatures of dispersing spin and charge excitations, which can be used to infer the nature of the underlying electron-electron interactions. In the case of CDW states with repulsive interactions we find a spin mode and a linear dispersing charge mode, while for attractive interactions a third dispersing mode appears, which can be thought of as arising from a spin excitation with a fixed momentum q_0 and a charge excitation with momentum $q - q_0$.

We have also investigated the modification of the LDOS due to boundary bound states. These may arise in the presence of boundary potentials or magnetic fields. We found that boundary bound states give rise to nondispersing singularities at energies below the single-particle gap. While the bound state is formed in the gapped sector of the theory, the exponent of the corresponding singularity depends only on the Luttinger liquid parameter of the gapless sector. We have analyzed temperature effects in regime $T \ll \Delta$ and discussed implications of our results for STM measurements on quasi-1D materials such as doped two-leg ladders.

ACKNOWLEDGMENTS

We would like to thank Joe Bhaseen, Dmitry Kovrizhin, and Christian Pfleiderer for useful discussions. D.S. was supported by the Deutsche Akademie der Naturforscher Leopoldina under Grant No. BMBF-LPD 9901/8-145 while working at the Rudolf Peierls Centre for Theoretical Physics, University of Oxford. This work was also supported by the EPSRC under Grant No. EP/D050952/1 (F.H.L.E.), the NSF under Grant No. DMR 0758462 at the University of Illinois (E.F.), the US Department of Energy, Division of Materials Sciences, under Grant No. DE-FG02-07ER46453 through the Frederick Seitz Materials Research Laboratory of the University of Illinois (E.F., A.J.) and the ESF network INSTANS.

APPENDIX A: RENORMALIZATION GROUP ANALYSIS OF AN IMPURITY POTENTIAL

Let us consider the low-energy theory of a 1D CDW state on the infinite line $H = H_c + H_s$, where

$$H_c = \frac{v_c}{16\pi}\int_{-\infty}^{\infty} dx \left[\frac{1}{K_c^2}(\partial_x \Phi_c)^2 + K_c^2(\partial_x \Theta_c)^2\right], \quad \text{(A1)}$$

$$H_s = \frac{v_s}{16\pi}\int_{-\infty}^{\infty} dx \left[\frac{1}{K_s^2}(\partial_x \Phi_s)^2 + K_s^2(\partial_x \Theta_s)^2\right] - \frac{g_s}{(2\pi)^2}\int_{-\infty}^{\infty} dx \cos\Phi_s. \quad \text{(A2)}$$

We want to study the effect of an impurity potential at position $x = 0$, which, in bosonized form, reads

$$V_{\rm imp} = \lambda \int_{-\infty}^{\infty} dx\, \delta(x) \cos\left(\frac{\Phi_c}{2}\right)\cos\left(\frac{\Phi_s}{2}\right). \quad \text{(A3)}$$

As the spin sector in the bulk is massive, we have $\langle\cos(\Phi_s/2)\rangle \neq 0$, which implies that at low energies we can approximate $\cos(\Phi_c/2)\cos(\Phi_s/2)$ in Eq. (A3) by $\langle\cos(\Phi_c/2)\rangle\cos(\Phi_s/2) + \cos(\Phi_c/2)\langle\cos(\Phi_s/2)\rangle$. Thus in the charge sector we get a boundary sine-Gordon model.[62] For $K_c^2 < 2$ the impurity scattering potential scales to strong coupling. Hence as long as the interactions are not too attractive, the field Φ_c gets pinned at the boundary, $\Phi_c(0) = 0$. This in turn induces an impurity contribution in the gapped spin sector

$$V_{\rm imp,s} = \lambda \left\langle\cos\left(\frac{\Phi_c(0)}{2}\right)\right\rangle \int_{-\infty}^{\infty} dx\, \delta(x)\cos\left(\frac{\Phi_s}{2}\right). \quad \text{(A4)}$$

If one analyzes the bulk and boundary cosine terms in the resulting impurity model, Eqs. (A2) and (A4), simultaneously,

the leading order renormalization group equations are given by the scaling dimensions of the perturbing operators:

$$\frac{dg_s}{dl} = 2\left(1 - K_s^2\right) g_s, \quad \frac{d\lambda}{dl} = \left(1 - \frac{K_s^2}{2}\right)\lambda. \tag{A5}$$

As long as $K_s^2 > 2/3$ the boundary term grows more rapidly than the bulk term. Assuming that it reaches the strong-coupling regime first leads to the pinning of the spin field $\Phi_s(0) = 0$. This cuts the chain in two half-lines and we obtain the model, Eqs. (12)–(15).

APPENDIX B: CALCULATION OF THE GREEN FUNCTION: CHARGE SECTOR

The Green function, Eq. (16), factorizes into a product of correlation functions in the spin and charge sectors. For example, using the bosonization identities, Eqs. (7) and (8), the $2k_F$-component $G^{RL}_{\sigma\sigma'}$ can be written as

$$G^{RL}_{\sigma\sigma'}(\tau,x_1,x_2) = -\frac{1}{2\pi}\left\langle e^{-\frac{i}{2}\phi_c(\tau,x_1)}\, e^{-\frac{i}{2}\bar\phi_c(0,x_2)}\right\rangle_c \times \left\langle e^{-\frac{i}{2}f_\sigma\phi_s(\tau,x_1)}\, e^{-\frac{i}{2}f_{\sigma'}\bar\phi_s(0,x_2)}\right\rangle_s. \tag{B1}$$

Both correlation functions have to be determined in the presence of the boundary at $x = 0$. The charge part is calculated here using a standard mode expansion;[36] the spin part is calculated in Appendix C.

To obtain the correlation functions in the charge sector, we first bring the Hamiltonian, Eq. (13), to standard form by rescaling the fields as $\Phi_c \to K_c\Phi_c$, $\Theta_c \to \Theta_c/K_c$. The charge parts of the operators, Eqs. (7) and (8), then become

$$\begin{aligned}&\exp\left(\pm\frac{i}{2}\phi_c(\tau,x)\right)\\ &\quad\to e^{i\pi sc/4}\exp\left(\pm\frac{i}{2}c\,\phi_c(z)\right)\exp\left(\pm\frac{i}{2}s\,\bar\phi_c(\bar z)\right)\\ &\quad= e^{-i\pi sc/4}\exp\left(\pm\frac{i}{2}s\,\bar\phi_c(\bar z)\right)\exp\left(\pm\frac{i}{2}c\,\phi_c(z)\right),\end{aligned} \tag{B2}$$

$$\begin{aligned}&\exp\left(\pm\frac{i}{2}\bar\phi_c(\tau,x)\right)\\ &\quad\to e^{i\pi sc/4}\exp\left(\pm\frac{i}{2}s\,\phi_c(z)\right)\exp\left(\pm\frac{i}{2}c\,\bar\phi_c(\bar z)\right)\\ &\quad= e^{-i\pi sc/4}\exp\left(\pm\frac{i}{2}c\,\bar\phi_c(\bar z)\right)\exp\left(\pm\frac{i}{2}s\,\phi_c(z)\right),\end{aligned} \tag{B3}$$

where we have already used Eq. (B7) and assumed $-L < x < 0$. The constants are parameterized via $s = \sinh\xi_c$ and $c = \cosh\xi_c$, with $K_c = e^{\xi_c}$. The complex coordinates are defined as $z = v_c\tau - ix$, $\bar z = v_c\tau + ix$. The charge part of the Green function can hence be obtained from the four-point function,

$$\langle e^{i\beta_1\bar\phi_c(\bar z_1)}\, e^{i\alpha_1\phi_c(z_1)}\, e^{i\alpha_2\phi_c(z_2)}\, e^{i\beta_2\bar\phi_c(\bar z_2)}\rangle_{\mathrm{UHP}}, \tag{B4}$$

where $\alpha_{1,2},\beta_{1,2} \in \mathbb{R}$, $z_1 = v_c\tau - ix_1$, and $z_2 = -ix_2$ lie in the upper half-plane.

We calculate Eq. (B4) from the mode expansions for the chiral fields ϕ_c and $\bar\phi_c$. These are obtained by first noting that the fields Φ_c and Θ_c have to satisfy the equations of motion $v_c\partial_x\Theta_c = -i\partial_\tau\Phi_c$ and $\partial_\tau\Theta_c = iv_c\partial_x\Phi_c$ as well as the boundary conditions $\Phi_c(x = 0) = \Phi_c(x = -L) = 0$. The semi-infinite system is obtained by taking $L \to \infty$. This yields the mode expansions

$$\Phi_c(\tau,x) = -\frac{x}{L}\hat\Pi_0 + i\sum_{n=1}^{\infty}\frac{\sin\frac{n\pi x}{L}}{\sqrt{n\pi}}\left(b_n\, e^{-n\pi v_c\tau/L} - b_n^\dagger\, e^{n\pi v_c\tau/L}\right), \tag{B5}$$

$$\Theta_c(\tau,x) = \hat\Theta_0 - i\,\frac{v_c\tau}{L}\hat\Pi_0 + \sum_{n=1}^{\infty}\frac{\cos\frac{n\pi x}{L}}{\sqrt{n\pi}} \times\left(b_n\, e^{-n\pi v_c\tau/L} + b_n^\dagger\, e^{n\pi v_c\tau/L}\right), \tag{B6}$$

where the zero-mode operator $\hat\Pi_0$ has the discrete spectrum $2\pi m$, $m \in \mathbb{Z}$, and $[\hat\Theta_0,\hat\Pi_0] = 8\pi i$, $[b_m,b_n^\dagger] = 8\pi\,\delta_{mn}$. The mode expansions for the chiral fields are easily obtained via $\phi_c = (\Phi_c + \Theta_c)/2$ and $\bar\phi_c = (\Phi_c - \Theta_c)/2$. Their commutation relations are

$$[\phi_c(\tau,x),\bar\phi_c(\tau,x')] = \begin{cases} 0, & x = x' = 0,\\ 4\pi i, & x = x' = -L,\\ 2\pi i, & \text{otherwise,}\end{cases} \tag{B7}$$

as well as $[\phi_c(\tau,x),\phi_c(\tau,x')] = -[\bar\phi_c(\tau,x),\bar\phi_c(\tau,x')] = 2\pi i\,\mathrm{sgn}(x - x')$, where $\mathrm{sgn}(0) = 0$. Similar mode expansions were obtained in Ref. 36. Given the mode expansion, it is straightforward to calculate the four-point function, Eq. (B4). We find

$$\begin{aligned}&\langle e^{i\beta_1\bar\phi_c(\bar z_1)}\, e^{i\alpha_1\phi_c(z_1)}\, e^{i\alpha_2\phi_c(z_2)}\, e^{i\beta_2\bar\phi_c(\bar z_2)}\rangle_{\mathrm{UHP}}\\ &= \frac{C\delta_{\alpha_1+\alpha_2,\beta_1+\beta_2}\,(z_1 - z_2)^{2\alpha_1\alpha_2}\,(\bar z_1 - \bar z_2)^{2\beta_1\beta_2}}{(\bar z_1 - z_1)^{2\alpha_1\beta_1}(\bar z_1 - z_2)^{2\alpha_2\beta_1}(z_1 - \bar z_2)^{2\alpha_1\beta_2}(z_2 - \bar z_2)^{2\alpha_2\beta_2}},\end{aligned} \tag{B8}$$

where $C \in \mathbb{R}$ is a constant that we set to 1 throughout this paper. This result implies Eq. (19). The finite-temperature correlation functions are obtained[38,58] by mapping Eq. (B8) onto a cylinder of circumference v_c/k_BT.

APPENDIX C: CALCULATION OF THE GREEN FUNCTION: SPIN SECTOR

The calculation of the correlation functions in the spin sector relies on the integrability of the sine-Gordon model on the half-line. We use the boundary-state formalism introduced by Ghoshal and Zamolodchikov[29] together with a form-factor expansion based on form factors obtained by Lukyanov and Zamolodchikov.[42] The analogous expansion for the quantum Ising model was analyzed in Ref. 48. We first discuss the general formalism and then derive Eq. (20).

1. Boundary-state formalism and form-factor expansion

Let us consider the sine-Gordon model, Eq. (14), in the half-plane (τ,x), $\tau \in \mathbb{R}$, $-\infty < x \leqslant 0$. The boundary is located at $x = 0$ and τ denotes imaginary time ($\tau = it$). The Hilbert space of states associated with the semi-infinite line $\tau = \mathrm{const}$, $-\infty < x \leqslant 0$, is denoted $\mathcal{H}_b$. We obtain the Euclidean action in its standard form by rescaling the fields according to $\Phi_s \to \Phi_s' = \Phi_s/K_s$ and $\Theta_s \to \Theta_s' = K_s\Theta_s$. The action of the

sine-Gordon model with a boundary is then given by[29] (we set $v_s = 1$)

$$\mathcal{S}_{\mathrm{bsG}} = \frac{1}{16\pi}\int d\tau \int_{-\infty}^{0} dx \times\left[(\partial_\tau\Phi_s')^2 + (\partial_x\Phi_s')^2 - \frac{4g_s}{\pi}\cos(K_s\Phi_s')\right] - g_b\int d\tau\,\cos\left(\frac{K_s}{2}(\Phi_s'|_{x=0} - \Phi_s^0/K_s)\right), \quad \text{(C1)}$$

where g_s, g_b, and Φ_s^0 are free parameters. (We use the conventions $0 < K_s < 1$; the action as given in Ref. 29 is obtained by another rescaling of the fields by $\sqrt{8\pi}$.) The cases $g_b = 0$ and $g_b \to \infty$ correspond to free and fixed boundary conditions, respectively. We stress that in the case of fixed boundary conditions, $\Phi_s'(x=0) = \Phi_s^0/K_s$ implies $\Phi_s(x=0) = \Phi_s^0$ in the original system, Eq. (14). As conjectured by Ghoshal and Zamolodchikov[29] and shown independently[30] by MacIntyre and Saleur *et al.*, the classical sine-Gordon model on the half-line, Eq. (C1), possesses infinitely many integrals of motion and is hence integrable.

We start by summarizing some results for the *bulk* sine-Gordon model, that is, the theory without boundary. In the repulsive regime ($K_s > 1/\sqrt{2}$) a basis of the Hilbert space $\mathcal{H}$ is given by scattering states of solitons and antisolitons

$$|\theta_1,\ldots,\theta_n\rangle_{a_1,\ldots,a_n} = Z_{a_1}^\dagger(\theta_1)\cdots Z_{a_n}^\dagger(\theta_n)|0\rangle,$$
$$ {}_{a_n,\ldots,a_1}\langle\theta_n,\ldots,\theta_1| = \langle 0|Z_{a_n}(\theta_n)\cdots Z_{a_1}(\theta_1), \quad \text{(C2)}$$

where $a_i = \pm 1$ and $|0\rangle$ is the ground state in the absence of a boundary. Solitons and antisolitons are created by the operators $Z_-^\dagger(\theta)$ and $Z_+^\dagger(\theta)$. They are characterized by a topological U(1) charge of -1 and 1, respectively, while their energy and momentum are parametrized in terms of the rapidity θ by $E = \Delta\cosh\theta$ and $P = \Delta\sinh\theta$. The dependence of the soliton mass Δ on the bare parameters in the action was obtained in Ref. 64. We note that in the attractive regime ($K_s < 1/\sqrt{2}$), breather (soliton-antisoliton) bound states occur as well. The operators Z_a and $Z_a^\dagger$ fulfill the Faddeev–Zamolodchikov algebra[65] (see Fig. 13):

$$\begin{aligned} Z_{a_1}(\theta_1)Z_{a_2}(\theta_2) &= S_{a_1a_2}^{b_1b_2}(\theta_1-\theta_2)Z_{b_2}(\theta_2)Z_{b_1}(\theta_1),\\ Z_{a_1}^\dagger(\theta_1)Z_{a_2}^\dagger(\theta_2) &= S_{a_1a_2}^{b_1b_2}(\theta_1-\theta_2)Z_{b_2}^\dagger(\theta_2)Z_{b_1}^\dagger(\theta_1),\\ Z_{a_1}(\theta_1)Z_{a_2}^\dagger(\theta_2) &= 2\pi\delta(\theta_1-\theta_2)\delta_{a_1a_2}\\ &\quad + S_{a_2b_1}^{b_2a_1}(\theta_1-\theta_2)Z_{b_2}^\dagger(\theta_2)Z_{b_1}(\theta_1). \end{aligned} \quad \text{(C3)}$$

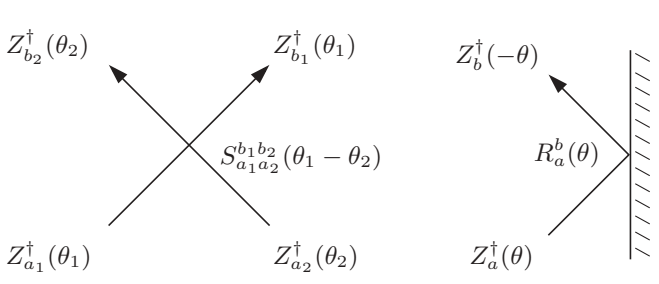

FIG. 13. Two-particle scattering and scattering off the boundary.

Here $S_{a_1a_2}^{b_1b_2}(\theta)$ is the two-particle scattering matrix, which was derived in Refs. 32 and 66. The unitarity condition reads $S_{a_1a_2}^{c_1c_2}(\theta)S_{c_1c_2}^{b_1b_2}(-\theta) = \delta_{a_1}^{b_1}\delta_{a_2}^{b_2}$. Its nonvanishing elements are

$$\begin{aligned} S_{++}^{++}(\theta) = S_{--}^{--}(\theta), \quad S_{+-}^{+-}(\theta) = S_{-+}^{-+}(\theta),\\ S_{-+}^{+-}(\theta) = S_{+-}^{-+}(\theta), \end{aligned} \quad \text{(C4)}$$

for which explicit expressions can be found, for example, in Ref. 44. At the LEP ($K_s = 1/\sqrt{2}$) the scattering matrix simplifies to $S_{a_1a_2}^{b_1b_2}(\theta) = -\delta_{a_1}^{b_1}\delta_{a_2}^{b_2}$, while in the spin symmetric case ($K_s = 1$), one has[46]

$$\begin{aligned} S_{++}^{++}(\theta) = S_0(\theta) &\equiv -\frac{\Gamma\left(1+\frac{i\theta}{2\pi}\right)\Gamma\left(\frac{1}{2}-\frac{i\theta}{2\pi}\right)}{\Gamma\left(1-\frac{i\theta}{2\pi}\right)\Gamma\left(\frac{1}{2}+\frac{i\theta}{2\pi}\right)},\\ S_{+-}^{+-}(\theta) = -\frac{\theta}{\theta-i\pi}S_0(\theta), &\quad S_{-+}^{+-}(\theta) = -\frac{i\pi}{\theta-i\pi}S_0(\theta). \end{aligned} \quad \text{(C5)}$$

We note that the Faddeev–Zamolodchikov algebra [Eq. (C3)] is invariant under the unitary transformation $Z_a(\theta) \to e^{i\varphi}Z_a(\theta)$, which changes the basis of scattering states. In terms of the basis states, Eq. (C2), the resolution of the identity reads

$$\mathrm{id} = |0\rangle\langle 0| + \sum_{n=1}^{\infty}\frac{1}{n!}\sum_{\{a_i\}}\int_{-\infty}^{\infty}\frac{d\theta_1\cdots d\theta_n}{(2\pi)^n} \times |\theta_n,\ldots,\theta_1\rangle_{a_n,\ldots,a_1}{}^{a_1,\ldots,a_n}\langle\theta_1,\ldots,\theta_n|. \quad \text{(C6)}$$

The boundary can be introduced[29] as an infinitely heavy, impenetrable particle B sitting at $x = 0$. The ground state in the presence of the boundary can then be represented as $|0_b\rangle = B|0\rangle$. Scattering of elementary excitations off the boundary is encoded in the relations (see Fig. 13)

$$Z_a^\dagger(\theta)B = R_a^b(\theta)Z_b^\dagger(-\theta)B, \quad \text{(C7)}$$

where the functions $R_a^b(\theta)$ are the single-particle reflection amplitudes. To preserve integrability, the boundary reflection matrix $R(\theta)$ has to satisfy a number of conditions, which are discussed in Ref. 29. At the LEP and for Dirichlet boundary conditions $\Phi_s(\tau, x=0) = \Phi_s^0$, $0 \leqslant \Phi_s^0 < \pi$ in the original system, Eq. (14), it is given by[45]

$$R_\pm^\pm(\theta) = -\frac{\cosh\left(i\frac{\pi}{4} \pm i\frac{\Phi_s^0}{2} + \frac{\theta}{2}\right)}{\cosh\left(i\frac{\pi}{4} \pm i\frac{\Phi_s^0}{2} - \frac{\theta}{2}\right)}, \quad R_\pm^\mp(\theta) = 0. \quad \text{(C8)}$$

For $\pi/2 \leqslant \Phi_s^0$ the reflection amplitude R_+^+ possesses a simple pole in the physical strip $0 \leqslant \Im\mathrm{m}\,\theta \leqslant \pi/2$, which indicates the existence of a boundary bound state. The overall sign of the reflection matrix is fixed by the requirement $-i\,\mathrm{Res}[R_\pm^\pm(\theta), \theta = \pm i(\Phi_s^0 \mp \pi/2)] = -2\cos\Phi_s^0 > 0$; see Sec. C 5. Explicit representations of R for general K_s are given in Refs. 29, 46, and 47. For $K_s = 1$ and $\Phi_s^0 = 0$ one finds, in particular,

$$\begin{aligned} R_\pm^\pm(\theta) = -\frac{\Gamma\left(1+\frac{i\theta}{2\pi}\right)\Gamma\left(\frac{1}{2}-\frac{i\theta}{\pi}\right)}{\sqrt{\pi}\,\Gamma\left(1-\frac{i\theta}{2\pi}\right)}2^{\frac{i}{\pi}\theta}\left(\cosh\frac{\theta}{2} + i\sinh\frac{\theta}{2}\right),\\ R_\pm^\mp(\theta) = 0. \end{aligned} \quad \text{(C9)}$$

The vanishing of the off-diagonal amplitudes $R_\pm^\mp(\theta) = 0$ is a consequence of fixed boundary conditions and holds for general K_s.

Our aim is to calculate the time-ordered two-point function:

$$C(\tau,x_1,x_2) = \langle 0_{\rm b}|\, \mathcal{T}_\tau\, O_1(\tau,x_1)\, O_2(0,x_2)\, |0_{\rm b}\rangle\,. \quad \text{(C10)}$$

Here the time dependence of the operators is given by $O_i(\tau,x) = e^{\tau H_{\rm b}}\, O_i(0,x)\, e^{-\tau H_{\rm b}}$, where $H_{\rm b}$ is the Hamiltonian of the system in the presence of the boundary, Eq. (14). Given that in the Euclidean formalism, τ and x are interchangeable, one may equally well designate x to be the "Euclidean time." In this picture the equal-time section is the infinite line, $x = \text{const}$, $-\infty < \tau < \infty$, and the associated Hilbert space $\mathcal{H}$ is that of the corresponding *bulk theory*. The boundary at $x = 0$ now appears as an initial condition that is expressed in terms of a "boundary state" $|{\rm B}\rangle$. It was shown by Ghoshal and Zamolodchikov[29] that the correlation function, Eq. (C10), can be expressed as

$$C(\tau,x_1,x_2) = e^{-{\rm i}\frac{\pi}{2}\sum_i s(O_i)}\, \frac{\langle 0|\, \mathcal{T}_x\, O_1(\tau,x_1)\, O_2(0,x_2)\, |{\rm B}\rangle}{\langle 0|\, {\rm B}\rangle}. \quad \text{(C11)}$$

Here $s(O_i)$ denotes the Lorentz spin of the operator O_i, $\mathcal{T}_x$ is the x-ordering operator, which orders the largest x_i to the right, and $|0\rangle \in \mathcal{H}$ is the ground state of the model on the infinite line. The spin-dependent phase factor is due to the rotation in Euclidean space; it was, for example, observed in the Green function of the Ising model with a boundary magnetic field.[48] As we have interchanged space and time and x is running from 0 to $-\infty$ in the new framework, the τ and x dependence of operators $O_i(\tau,x)$ is now given by

$$O_i(\tau,x) = e^{-xH}\, e^{-{\rm i}\tau P}\, O_i(0,0)\, e^{{\rm i}\tau P}\, e^{xH}, \quad \text{(C12)}$$

where H is the Hamiltonian of the system on the infinite line $-\infty < \tau < \infty$, and P is the total momentum.

The boundary state, which encodes all information on the boundary condition, is given by

$$|{\rm B}\rangle = \exp\left(\frac{1}{2}\int_{-\infty}^{\infty}\frac{d\xi}{2\pi}K^{ab}(\xi)Z_a^\dagger(-\xi)Z_b^\dagger(\xi)\right)|0\rangle\,, \quad \text{(C13)}$$

where $K^{ab}(\xi) = R_a^b({\rm i}\pi/2 - \xi)$. For example, the boundary reflection amplitudes K stated in Eqs. (21) and (38) are directly obtained from Eqs. (C8) and (C9). For general $K_{\rm s}$ the amplitude K^{ab} satisfies the boundary cross-unitarity condition,[29]

$$K^{ab}(\xi) = S_{cd}^{ab}(2\xi)\, K^{dc}(-\xi). \quad \text{(C14)}$$

Furthermore, for fixed boundary conditions we have $K^{\pm\pm}(\xi) = 0$.

Here we calculate the spin part of the Green function, Eq. (B1), using the boundary formalism already presented. Specifically we evaluate the correlation function, Eq. (C11), where the operators $O_{1,2}$ are the soliton-creating and -annihilating operators $e^{\pm\frac{\rm i}{2}\phi_{\rm s}}$ and $e^{\pm\frac{\rm i}{2}\bar\phi_{\rm s}}$, respectively. We define the n-particle form factor of an arbitrary operator O as

$$\begin{aligned} f^{O}_{a_1,\ldots,a_n}(\theta_1,\ldots,\theta_n) &= \langle 0|O|\theta_1,\ldots,\theta_n\rangle_{a_1,\ldots,a_n} \\ &= \langle 0|O\, Z^\dagger_{a_1}(\theta_1)\ldots Z^\dagger_{a_n}(\theta_n)|0\rangle. \end{aligned} \quad \text{(C15)}$$

The form factors have to satisfy a set of relations, the so-called form-factor axioms,[39,41,43] which we state for completeness in Sec. C 2. As the operators $e^{-\frac{\rm i}{2}\phi_{\rm s}}$ and $e^{\frac{\rm i}{2}\bar\phi_{\rm s}}$ create one soliton, their respective form factors, Eq. (C15), vanish unless $\sum_i a_i = -1$. The form factors containing up to three particles were derived by Lukyanov and Zamolodchikov.[42] In our conventions the single-particle form factors are given by

$$\begin{aligned} \langle 0|\, e^{-\frac{\rm i}{2}\phi_{\rm s}}\, |\theta\rangle_- &= \sqrt{Z_1}\, e^{{\rm i}\frac{\pi}{8}}\, e^{\theta/4}, \\ \langle 0|\, e^{\frac{\rm i}{2}\bar\phi_{\rm s}}\, |\theta\rangle_- &= \sqrt{Z_1}\, e^{-{\rm i}\frac{\pi}{8}}\, e^{-\theta/4}, \end{aligned} \quad \text{(C16)}$$

where the normalization constant Z_1 [not to be confused with the Faddeev–Zamolodchikov operators $Z_\pm(\theta)$ and $Z^\dagger_\pm(\theta)$] depends on $K_{\rm s}$ and is given in Ref. 42. Evaluation at the LEP yields $Z_1 \approx 3.320\,52\,\Delta^{5/8}$, whereas at the SU(2) invariant point, one finds $Z_1 \approx 0.921\,862\,\Delta^{1/2}$. The three-particle form factors are known in terms of contour integrals, which can be explicitly evaluated at the LEP:

$$\left.\begin{aligned} &\langle 0|\, e^{-\frac{\rm i}{2}\phi_{\rm s}}\, |\theta_1,\theta_2,\theta_3\rangle_{--+} \\ &\langle 0|\, e^{\frac{\rm i}{2}\bar\phi_{\rm s}}\, |\theta_1,\theta_2,\theta_3\rangle_{--+} \end{aligned}\right\} = -{\rm i}\sqrt{\frac{Z_1}{2}}\, e^{\pm{\rm i}\frac{\pi}{8}}\, e^{\pm(\theta_1+\theta_2-\theta_3)/4} \times \frac{\sinh\frac{\theta_1-\theta_2}{2}}{\cosh\frac{\theta_1-\theta_3}{2}\cosh\frac{\theta_2-\theta_3}{2}}. \quad \text{(C17)}$$

The three-particle form factors for other orderings of the U(1) indices can be easily obtained using the scattering axiom stated in Sec. C 2.

The correlation functions calculated here contain matrix elements with incoming and outgoing particles,

$$ {}_{a_1,\ldots,a_n}\langle\theta_1,\ldots,\theta_n|\, O\, |\xi_m,\ldots,\xi_1\rangle_{b_m,\ldots,b_1}\,, \quad \text{(C18)}$$

which possess kinematical poles whenever $\theta_i = \xi_j$ and $a_i = b_j$. These matrix elements can be decomposed into "connected" and "disconnected" contributions. The latter are characterized by the appearance of terms like $\delta(\theta_i - \xi_j)$, signaling that some of the particles do not encounter the operator O in the process described by the matrix element. We deal with these terms following ideas by Smirnov[39] that allow us to analytically continue form factors. Let $\overrightarrow{A} = \{\theta_1,\ldots,\theta_n\}$ with $\theta_1 < \theta_2 < \cdots < \theta_n$ and $\overleftarrow{B} = \{\xi_m,\ldots,\xi_1\}$ with $\xi_m > \xi_{m-1} > \cdots > \xi_1$ denote two sets of ordered rapidities and introduce the notations

$$Z[\overrightarrow{A}\,]_{a_1\cdots a_n} \equiv Z_{a_1}(\theta_1)Z_{a_2}(\theta_2),\ldots,Z_{a_n}(\theta_n), \quad \text{(C19)}$$

$$Z^\dagger[\overleftarrow{B}\,]_{b_m,\ldots,b_1} \equiv Z^\dagger_{b_m}(\xi_m)Z^\dagger_{b_{m-1}}(\xi_{m-1})\cdots Z^\dagger_{b_1}(\xi_1). \quad \text{(C20)}$$

Now let A_1 and A_2 be a partition of A, that is, $A = A_1 \cup A_2$, where A_1 contains $n(A_1) = n - k$ rapidities. As a consequence of the Faddeev–Zamolodchikov algebra, we have

$$Z[\overrightarrow{A}\,]_{a_1\cdots a_n} = S(\overrightarrow{A}\,|\overrightarrow{A_1})^{c_1\cdots c_n}_{a_1\cdots a_n}\, Z[\overrightarrow{A_2}]_{c_1\cdots c_k}\, Z[\overrightarrow{A_1}]_{c_{k+1}\cdots c_n}, \quad \text{(C21)}$$

where $S(\overrightarrow{A}\,|\overrightarrow{A_1})$ is the product of two-particle scattering matrixes needed to rearrange the order of Faddeev–Zamolodchikov operators in $Z[\overrightarrow{A}\,]$ to arrive at $Z[\overrightarrow{A_2}]Z[\overrightarrow{A_1}]$. For example, if $\overrightarrow{A} = \{\theta_1,\ldots,\theta_4\}$ and $\overrightarrow{A_1} = \{\theta_2,\theta_3\}$ it is given by

$$S(\overrightarrow{A}\,|\overrightarrow{A_1})^{c_1\cdots c_4}_{a_1\cdots a_4} = \delta^{c_4}_{a_1}\, S^{c_2c_4}_{a_2b}(\theta_2-\theta_4)\, S^{c_3b}_{a_3a_4}(\theta_3-\theta_4). \quad \text{(C22)}$$

Similarly we have

$$Z^\dagger[\overleftarrow{B}]_{b_m,\ldots,b_1} = Z^\dagger[\overleftarrow{B_1}]_{d_m\ldots d_{l+1}} Z^\dagger[\overleftarrow{B}_2]_{d_l\cdots d_1}\; S(\overleftarrow{B_1}|\overleftarrow{B})^{d_m\cdots d_1}_{b_m\cdots b_1}. \tag{C23}$$

Finally, we define

$$\delta[\overrightarrow{A},\overleftarrow{B}]^{a_1\cdots a_n}_{b_m\cdots b_1} = \delta_{nm}\prod_{j=1}^{n} 2\pi\,\delta_{a_j b_j}\delta(\theta_j-\xi_j). \tag{C24}$$

We are now in the position to analytically continue matrix elements as

$$\begin{aligned}&\langle 0|Z[\overrightarrow{A}]_{a_1\cdots a_n}\, O\, Z^\dagger[\overleftarrow{B}]_{b_m\cdots b_1}|0\rangle\\ &\quad=\sum_{\substack{A=A_1\cup A_2\\ B=B_1\cup B_2}} S(\overrightarrow{A}|\overrightarrow{A_1})^{c_1\cdots c_n}_{a_1\cdots a_n}\, S(\overleftarrow{B_1}|\overleftarrow{B})^{d_m\cdots d_1}_{b_m\cdots b_1}\,\delta[\overrightarrow{A_2},\overleftarrow{B_2}]^{c_1\cdots c_k}_{d_l\cdots d_1}\\ &\qquad\times\langle 0|Z[\overrightarrow{A}_1+\mathrm{i}0]_{c_{k+1}\cdots c_n}\, O\, Z^\dagger[\overleftarrow{B}_1]_{d_m\cdots d_{l+1}}|0\rangle.\end{aligned} \tag{C25}$$

Here the sum is over all possible ways to break sets A and B into subsets, and $\overrightarrow{A}_1+\mathrm{i}0$ means that all rapidities in A_1 are slightly moved into the upper half-plane. Similarly, we could choose to analytically continue to the lower half-plane,

$$\begin{aligned}&\langle 0|Z[\overrightarrow{A}]_{a_1\ldots a_n}\, O\, Z^\dagger[\overleftarrow{B}]_{b_m\ldots b_1}|0\rangle\\ &\quad=\sum_{\substack{A=A_1\cup A_2\\ B=B_1\cup B_2}} d_{A_2}(O)\, S(\overrightarrow{A}|\overrightarrow{A_2})^{c_1\ldots c_n}_{a_1\ldots a_n}\, S(\overleftarrow{B_2}|\overleftarrow{B})^{d_m\ldots d_1}_{b_m\ldots b_1}\,\delta[\overrightarrow{A_2},\overleftarrow{B_2}]^{c_1\ldots c_k}_{d_l\ldots d_1}\\ &\qquad\times\langle 0|Z[\overrightarrow{A}_1-\mathrm{i}0]_{c_{k+1}\ldots c_n}\, O\, Z^\dagger[\overleftarrow{B}_1]_{d_m\ldots d_{l+1}}|0\rangle.\end{aligned} \tag{C26}$$

The factor $d_{A_2}(O)$ is due to a possible semilocality of the operator O with respect to the fundamental fields creating the excitations.[39,41,43,52] If we use the operators $O_0^\pm$ defined in Eq. (C29) as fundamental fields and denote the mutual semilocality factor of O and $O_0^\pm$ by $l_\pm(O)$, it is given by

$$\begin{aligned}&d_A(O)=\prod_{i=1}^{n(A)} l_{a_i}(O) \quad\Rightarrow\quad d_{A_2}\big(e^{-\frac{\mathrm{i}}{2}\phi_s}\big)=\prod_{i=1}^{k} e^{-\mathrm{i}\frac{\pi}{2}a_i},\\ &\qquad\qquad d_{A_2}\big(e^{\frac{\mathrm{i}}{2}\bar\phi_s}\big)=\prod_{i=1}^{k} e^{\mathrm{i}\frac{\pi}{2}a_i}.\end{aligned} \tag{C27}$$

The remaining matrix elements in Eqs. (C25) and (C26) can be evaluated using crossing

$$\begin{aligned}&\langle 0|Z[\overrightarrow{A}_1\pm\mathrm{i}0]_{c_{k+1},\ldots,c_n}\, O\, Z^\dagger[\overleftarrow{B}_1]_{d_m,\ldots,d_{l+1}}|0\rangle\\ &\quad={}^{c_{k+1},\ldots,c_n}\big\langle\theta_{i_{k+1}}\pm\mathrm{i}0,\ldots,\theta_{i_n}\pm\mathrm{i}0\big|\, O\,\big|\xi_{j_m},\ldots,\xi_{j_{l+1}}\big\rangle_{d_m,\ldots,d_{l+1}}\\ &\quad=d_{A_1}(O)\,C_{c_{k+1}e_{k+1}}\cdots C_{c_ne_n}\\ &\qquad\times f^O_{e_{k+1},\ldots,e_n,d_m,\ldots,d_{l+1}}\big(\theta_{i_{k+1}}+\mathrm{i}\pi\pm\mathrm{i}\eta_{i_{k+1}},\ldots,\\ &\qquad\quad\theta_{i_n}+\mathrm{i}\pi\pm\mathrm{i}\eta_{i_n},\xi_{j_m},\ldots,\xi_{j_{l+1}}\big),\end{aligned} \tag{C28}$$

where $C_{ab}=\delta_{a+b,0}$ is the charge conjugation matrix and $\eta_i\to 0+$. The analytic continuation of general matrix elements, Eq. (C18), with arbitrary orders of the rapidities can be obtained using the scattering axiom (see the following).

2. Form-factor axioms

For completeness we state here the used form-factor axioms. We follow Delfino.[43] The n-particle form factor of an arbitrary operator O is defined in Eq. (C15). We use the local bosonic fields,

$$O_0^\pm(\tau,x)=\exp\left(\mp\frac{1}{4K_s}\int_{-\infty}^{\tau} d\tau\;\partial_x\,\Phi_s'(\tau,x)\right), \tag{C29}$$

as fundamental fields for the creation of solitons and antisolitons. The corresponding creation and annihilation operators are $Z_\pm^\dagger(\theta)$ and $Z_\pm(\theta)$, introduced in Eq. (C2). The form-factor axioms read as follows.

(1) The form factors $f^O_{a_1,\ldots,a_n}(\theta_1,\ldots,\theta_n)$ are meromorphic functions of θ_n in the physical strip $0\leqslant\Im\mathrm{m}\,\theta_n\leqslant 2\pi$. There exist only simple poles in this strip.

(2) The scattering axiom is

$$\begin{aligned}&f^O_{a_1,\ldots,a_i,a_{i+1},\ldots,a_n}(\theta_1,\ldots,\theta_i,\theta_{i+1},\ldots,\theta_n)\\ &\quad=S^{b_ib_{i+1}}_{a_ia_{i+1}}(\theta_i-\theta_{i+1})\, f^O_{a_1,\ldots,b_{i+1},b_i,\ldots,a_n}(\theta_1,\ldots,\theta_{i+1},\theta_i,\ldots,\theta_n),\end{aligned}$$

with the scattering matrix $S^{b_ib_{i+1}}_{a_ia_{i+1}}(\theta_i-\theta_{i+1})$. At the free-fermion point it is given by $S^{b_1b_2}_{a_1a_2}(\theta)=-\delta^{b_1}_{a_1}\delta^{b_2}_{a_2}$.

(3) The periodicity axiom is

$$f^O_{a_1,\ldots,a_n}(\theta_1+2\pi\mathrm{i},\theta_2,\ldots,\theta_n)=l_{a_1}(O)\, f^O_{a_2,\ldots,a_n,a_1}(\theta_2,\ldots,\theta_n,\theta_1),$$

where $l_\pm(O)$ is the mutual semilocality factor between the operator O and the fundamental fields $O_0^\pm$. In particular, we have $l_\pm(e^{-\frac{\mathrm{i}}{2}\phi_s})=\mp\mathrm{i}$ and $l_\pm(e^{\frac{\mathrm{i}}{2}\bar\phi_s})=\pm\mathrm{i}$.

(4) The Lorentz transformations are

$$f^O_{a_1,\ldots,a_n}(\theta_1+\Lambda,\ldots,\theta_n+\Lambda)=e^{s(O)\Lambda}\, f^O_{a_1,\ldots,a_n}(\theta_1,\ldots,\theta_n),$$

where $s(O)$ denotes the Lorentz spin of O. Here we have $s(e^{\pm\frac{\mathrm{i}}{2}\phi_s})=1/4$ and $s(e^{\pm\frac{\mathrm{i}}{2}\bar\phi_s})=-1/4$.

(5) The annihilation pole axiom is

$$\begin{aligned}&\mathrm{Res}\big[f^O_{a,b,a_1,\ldots,a_n}(\theta',\theta,\theta_1,\ldots,\theta_n),\theta'=\theta+\mathrm{i}\pi\big]\\ &\quad=\mathrm{i}\,C_{ac}\, f^O_{b_1,\ldots,b_n}(\theta_1,\ldots,\theta_n)\\ &\qquad\times\big[\delta^{b_1}_{a_1}\cdots\delta^{b_n}_{a_n}\delta^c_b-l_a(O)S^{c\ b_1}_{c_1a_1}(\theta-\theta_1)\\ &\qquad\quad\times S^{c_1b_2}_{c_2a_2}(\theta-\theta_2)\cdots S^{c_{n-1}b_n}_{b\ a_n}(\theta-\theta_n)\big],\end{aligned}$$

with the charge conjugation matrix $C_{ab}=\delta_{a+b,0}$. If bound states do not exist in the model, that is, for $K_s^2\geqslant 1/2$, these are the only poles of the form factors.

We note that the precise form of the axioms depends on the basis of scattering states and thus changes under a unitary transformation of the operators $Z_a(\theta)$.

3. Correlation functions

In this section we derive Eq. (20) using the boundary-state formalism. We start with the spin part of Eq. (B1). After the rotation in Euclidean space, this is given by Eq. (C11). We insert a resolution of the identity, Eq. (C6), and expand the boundary state, Eq. (C13), in powers of K. This yields the

double expansion ($\tau > 0$, $x_1 < x_2$)

$$\left\langle e^{-\frac{\mathrm{i}}{2} f_\sigma \phi_\mathrm{s}(\tau,x_1)}\, e^{-\frac{\mathrm{i}}{2} f_{\sigma'} \bar{\phi}_\mathrm{s}(0,x_2)} \right\rangle_\mathrm{s} = \langle 0|\, e^{-\frac{\mathrm{i}}{2} f_\sigma \phi_\mathrm{s}(\tau,x_1)}\, e^{-\frac{\mathrm{i}}{2} f_{\sigma'} \bar{\phi}_\mathrm{s}(0,x_2)}\, |\mathrm{B}\rangle = \delta_{\sigma\sigma'} \sum_{n=0}^{\infty}\sum_{m=0}^{\infty} C_{n\,2m}(\tau,x_1,x_2), \tag{C30}$$

where we have used $s(e^{\pm\frac{\mathrm{i}}{2}\phi_\mathrm{s}}) + s(e^{\pm\frac{\mathrm{i}}{2}\bar{\phi}_\mathrm{s}}) = 0$. The operators $e^{\pm\frac{\mathrm{i}}{2}\phi_\mathrm{s}}$ and $e^{\pm\frac{\mathrm{i}}{2}\bar{\phi}_\mathrm{s}}$ change the U(1) charge by ∓ 1 and ± 1, respectively. As the boundary state has vanishing U(1) charge for Dirichlet boundary conditions [$K^{\sigma\sigma}(\xi) = 0$], the correlation function is diagonal in spin space. Furthermore, we have defined the auxiliary functions

$$\begin{aligned} C_{n\,2m}(\tau,x_1,x_2) &= \frac{1}{2^m}\frac{1}{m!}\frac{1}{n!}\int_{-\infty}^{\infty}\frac{d\xi_1\cdots d\xi_m}{(2\pi)^m} \\ &\times \int_{-\infty}^{\infty}\frac{d\theta_1\cdots d\theta_n}{(2\pi)^n}\, K^{a_1 b_1}(\xi_1)\cdots K^{a_m b_m}(\xi_m) \\ &\times \langle 0|e^{-\frac{\mathrm{i}}{2} f_\sigma \phi_\mathrm{s}(\tau,x_1)}|\theta_n,\ldots,\theta_1\rangle_{c_n,\ldots,c_1} \\ &\times {}^{c_1,\ldots,c_n}\langle\theta_1,\ldots,\theta_n|e^{-\frac{\mathrm{i}}{2} f_\sigma \bar{\phi}_\mathrm{s}(0,x_2)}| \\ &\quad -\xi_1,\xi_1,\ldots,-\xi_m,\xi_m\rangle_{a_1,b_1,\ldots,a_m,b_m}. \end{aligned} \tag{C31}$$

We use the notations $\uparrow = +, \downarrow = -, \bar{\sigma} = -$ for $\sigma = +$, and vice versa. We label the various terms in the expansion, Eq. (C30), by the numbers of particles in the intermediate state n and in the boundary state $2m$, respectively. The τ and x dependence of the operators is given by Eq. (C12). We have already assumed $x_1 < x_2$ to avoid additional phases due to the mutual semilocality of the operators. For the calculation of the LDOS we have to take $x_1 \to x_2-$, finally. The second matrix element possesses kinematical poles that we treat using Eq. (C25). This introduces a third, finite summation in Eq. (C30), which labels the "connectedness" of the corresponding terms. We note, however, that Eqs. (C25) and (C26) yield the same results.

Let us start with the first nonvanishing term in the series, Eq. (C30), which, using Eq. (C12), is given by [we recall that the center-of-mass coordinates are defined by $R = (x_1 + x_2)/2 < 0$ and $r = x_1 - x_2 < 0$]

$$\begin{aligned} C_{10} &= \int_{-\infty}^{\infty}\frac{d\theta}{2\pi}\, \langle 0|\, e^{-\frac{\mathrm{i}}{2} f_\sigma \phi_\mathrm{s}}\, |\theta\rangle_c \\ &\quad \times {}^c\langle\theta|\, e^{-\frac{\mathrm{i}}{2} f_\sigma \bar{\phi}_\mathrm{s}}\, |0\rangle\; e^{\frac{\Delta}{v_\mathrm{s}} r\cosh\theta}\, e^{\mathrm{i}\Delta\tau\sinh\theta} \\ &= Z_1\, e^{\mathrm{i}\frac{\pi}{4}} \int_{-\infty}^{\infty}\frac{d\theta}{2\pi}\, e^{\frac{\Delta}{v_\mathrm{s}} r\cosh\theta}\, e^{\mathrm{i}\Delta\tau\sinh\theta}. \end{aligned} \tag{C32}$$

We can rewrite this by shifting the contour of integration as $\theta \to \theta + \mathrm{i}\pi/2$. The contributions of $\mathfrak{Re}\,\theta = \pm\infty$ vanish due to the exponential factors. As there are no poles in the strip $0 \leqslant \mathfrak{Im}\,\theta \leqslant \pi/2$, we find

$$\begin{aligned} C_{10} &= Z_1\, e^{\mathrm{i}\frac{\pi}{4}} \int_{-\infty}^{\infty}\frac{d\theta}{2\pi}\, e^{\mathrm{i}\frac{\Delta}{v_\mathrm{s}} r\sinh\theta}\, e^{-\Delta\tau\cosh\theta} \\ &= \frac{Z_1}{\pi}\, e^{\mathrm{i}\frac{\pi}{4}}\, K_0\big(\Delta\sqrt{\tau^2 + r^2/v_\mathrm{s}^2}\big), \end{aligned} \tag{C33}$$

where K_0 denotes the modified Bessel function.[63]

The first term containing the boundary reflection amplitude K is C_{12}. For $f_\sigma = -1$ it reads

$$\begin{aligned} C_{12} &= \frac{1}{2}\int_{-\infty}^{\infty}\frac{d\xi}{2\pi}\frac{d\theta}{2\pi}\, K^{ab}(\xi)\; \langle 0|\, e^{\frac{\mathrm{i}}{2}\phi_\mathrm{s}}\, |\theta\rangle_c \\ &\quad \times {}^c\langle\theta|\, e^{\frac{\mathrm{i}}{2}\bar{\phi}_\mathrm{s}}\, |-\xi,\xi\rangle_{ab}\; e^{\frac{\Delta}{v_\mathrm{s}} r\cosh\theta}\, e^{2\frac{\Delta}{v_\mathrm{s}} x_2\cosh\xi}\, e^{\mathrm{i}\Delta\tau\sinh\theta}. \end{aligned} \tag{C34}$$

The first form factor vanishes for $c \neq +$ and can be evaluated using Eq. (C28):

$$\begin{aligned} \langle 0|\, e^{\frac{\mathrm{i}}{2}\phi_\mathrm{s}}\, |\theta\rangle_+ &= {}^+\langle\theta|\, e^{-\frac{\mathrm{i}}{2}\phi_\mathrm{s}}\, |0\rangle^* \\ &= e^{\mathrm{i}\frac{\pi}{2}}\; \langle 0|\, e^{-\frac{\mathrm{i}}{2}\phi_\mathrm{s}}\, |\theta + \mathrm{i}\pi\rangle_-^* = \sqrt{Z_1}\, e^{\mathrm{i}\frac{\pi}{8}}\, e^{\theta/4}. \end{aligned} \tag{C35}$$

For the second matrix element we use Eq. (C25), which explicitly yields

$$\begin{aligned} {}^+\langle\theta|\, e^{\frac{\mathrm{i}}{2}\bar{\phi}_\mathrm{s}}\, |-\xi,\xi\rangle_{-+} &= {}^+\langle\theta + \mathrm{i}0|\, e^{\frac{\mathrm{i}}{2}\bar{\phi}_\mathrm{s}}\, |-\xi,\xi\rangle_{-+} \\ &\quad + 2\pi\delta(\theta-\xi)\, \langle 0|\, e^{\frac{\mathrm{i}}{2}\bar{\phi}_\mathrm{s}}\, |-\xi\rangle_- \\ &\quad + 2\pi\delta(\theta+\xi) S^{+-}_{-+}(-2\xi)\, \langle 0|\, e^{\frac{\mathrm{i}}{2}\bar{\phi}_\mathrm{s}}\, |\xi\rangle_-\,, \\ {}^+\langle\theta|\, e^{\frac{\mathrm{i}}{2}\bar{\phi}_\mathrm{s}}\, |-\xi,\xi\rangle_{+-} &= {}^+\langle\theta + \mathrm{i}0|\, e^{\frac{\mathrm{i}}{2}\bar{\phi}_\mathrm{s}}\, |-\xi,\xi\rangle_{+-} + 2\pi\delta(\theta+\xi) \\ &\quad \times S^{+-}_{+-}(-2\xi)\; \langle 0|\, e^{\frac{\mathrm{i}}{2}\bar{\phi}_\mathrm{s}}\, |\xi\rangle_-\,. \end{aligned} \tag{C36}$$

This leads to two contributions that we denote by C^0_{12} and C^1_{12}, respectively. The additional upper index denotes the number of lines connecting the operators (the "connectedness"), that is, the number of internal θ integrations left after using Eq. (C25). The first terms on the right-hand side of Eq. (C36), in each equation, together yield C^1_{12}. We calculate this term at the LEP in the next section. On the other hand, the disconnected piece is given by

$$\begin{aligned} C^0_{12} &= \frac{Z_1}{2}\int_{-\infty}^{\infty}\frac{d\xi}{2\pi}[K^{-+}(\xi) + K^{+-}(-\xi)\, S^{+-}_{+-}(2\xi) \\ &\quad + K^{-+}(-\xi)\, S^{+-}_{-+}(2\xi)]\, e^{\xi/2}\, e^{2\frac{\Delta}{v_\mathrm{s}} R\cosh\xi}\, e^{\mathrm{i}\Delta\tau\sinh\xi}. \end{aligned} \tag{C37}$$

Using the boundary cross-unitarity, Eq. (C14), the terms in the brackets equal $2K^{-+}(\xi)$. With a similar calculation for $f_\sigma = 1$, we arrive at

$$C^0_{12} = Z_1 \int_{-\infty}^{\infty}\frac{d\xi}{2\pi}\, K^{\sigma\bar{\sigma}}(\xi)\, e^{\xi/2}\, e^{2\frac{\Delta}{v_\mathrm{s}} R\cosh\xi}\, e^{\mathrm{i}\Delta\tau\sinh\xi}. \tag{C38}$$

The second term in Eq. (20) is now obtained by shifting the contour of integration as $\xi \to \xi + \mathrm{i}\pi/2$ while noting that, for the boundary condition $\Phi_\mathrm{s}(x=0) = 0$, the reflection amplitude does not depend on σ and is analytic in the physical strip $0 \leqslant \mathfrak{Im}\,\xi \leqslant \pi/2$. If $\Phi_\mathrm{s}(x=0) \neq 0$, however, the reflection amplitude may possess a pole in the physical strip. We calculate the resulting term in Sec. C 5.

4. Higher-order terms

To estimate the truncation error in Eq. (20), we calculate the leading corrections due to a higher number of particles in the intermediate state as well as higher-order corrections due to the boundary. The resulting corrections to the LDOS are discussed in Sec. IV C. We restrict ourselves to the LEP, where the form factors are given by Eq. (C17), $S^{b_1 b_2}_{a_1 a_2}(\theta) = -\delta^{b_1}_{a_1}\delta^{b_2}_{a_2}$, and $K^{ab}(\xi) = -K^{ba}(-\xi)$.

The leading correction due to a higher number of particles in the intermediate state is given by C_{30}:

$$C_{30} = Z_1 \frac{e^{i\frac{\pi}{4}}}{4} \int_{-\infty}^{\infty} \frac{d\theta_1 d\theta_2 d\theta_3}{(2\pi)^3} \frac{\sinh^2 \frac{\theta_1-\theta_2}{2}}{\cosh^2 \frac{\theta_1-\theta_3}{2} \cosh^2 \frac{\theta_2-\theta_3}{2}} \times e^{i\frac{\Delta}{v_s} r \sum_i \sinh\theta_i} e^{-\Delta\tau \sum_i \cosh\theta_i}. \quad \text{(C39)}$$

The resulting contribution to the LDOS, discussed in Sec. IV C, is denoted N_{30}. We note that $C_{20} = 0$.

The first subleading term due to the boundary is given by C^1_{12}, that is, the connected piece of C_{12} obtained from the first term in Eq. (C36). For $f_\sigma = -1$ this term reads, using (C35) and (C17),

$$C^1_{12} = Z_1 \frac{e^{-i\frac{\pi}{4}}}{\sqrt{2}} \int_{-\infty}^{\infty} \frac{d\xi}{2\pi} \frac{d\theta}{2\pi} \frac{K^{-+}(\xi)}{\cosh\xi} \frac{\sinh\frac{\theta+\xi+i\pi}{2}}{\cosh\frac{\theta-\xi+i\pi+i\eta}{2}} \times e^{\xi/2} e^{\frac{\Delta}{v_s} r\cosh\theta} e^{2\frac{\Delta}{v_s} x_2 \cosh\xi} e^{i\Delta\tau\sinh\theta}, \quad \text{(C40)}$$

where $\eta \to 0+$. We can handle the singularity at $\theta = \xi - i\eta$ by shifting $\theta \to \theta + i\pi/2$. Performing the same steps for $f_\sigma = 1$, we arrive at

$$C^1_{12} = Z_1 \frac{e^{-i\frac{\pi}{4}}}{\sqrt{2}} \int_{-\infty}^{\infty} \frac{d\xi}{2\pi} \frac{d\theta}{2\pi} \frac{K^{\sigma\bar\sigma}(\xi)}{\cosh\xi} \frac{e^{\xi+\theta} - i}{ie^{\xi} + e^{\theta}} \times e^{\xi/2} e^{i\frac{\Delta}{v_s} r\sinh\theta} e^{2\frac{\Delta}{v_s} x_2 \cosh\xi} e^{-\Delta\tau\cosh\theta}. \quad \text{(C41)}$$

The next term in the series, Eq. (C30), is C_{32}; its disconnected piece is similar to C^1_{12} and reads explicitly

$$C^1_{32} = -Z_1 \frac{e^{-i\frac{\pi}{4}}}{\sqrt{2}} \int_{-\infty}^{\infty} \frac{d\xi}{2\pi} \frac{d\theta}{2\pi} \frac{K^{\sigma\bar\sigma}(\xi)}{\cosh\xi} \frac{ie^{\xi} + e^{\theta}}{e^{\xi+\theta} - i} \times e^{\xi/2} e^{i\frac{\Delta}{v_s} r\sinh\theta} e^{2\frac{\Delta}{v_s} x_1 \cosh\xi} e^{-\Delta\tau\cosh\theta}. \quad \text{(C42)}$$

The terms C^1_{12} and C^1_{32} are of the same order and yield, together, the contribution to the LDOS denoted N_{11}.

The term resulting in N_{21} is

$$C^2_{32} = -\frac{Z_1}{2} e^{i\frac{\pi}{4}} \int_{-\infty}^{\infty} \frac{d\xi}{2\pi} \frac{d\theta_1 d\theta_2}{(2\pi)^2} e^{i\frac{\Delta}{v_s} r\sum_i \sinh\theta_i} e^{2i\frac{\Delta}{v_s} R\sinh\xi} e^{-\Delta\tau(\sum_i \cosh\theta_i + \cosh\xi)} \times \left[\frac{K^{\sigma\bar\sigma}\left(\xi + i\frac{\pi}{2}\right) e^{\xi/2}}{\cosh^2\frac{\theta_1-\theta_2}{2}} \frac{\sinh\frac{\xi-\theta_1}{2} \sinh\frac{\xi+\theta_1}{2}}{\cosh\frac{\xi-\theta_2}{2} \cosh\frac{\xi+\theta_2}{2}} - \frac{i}{2} \frac{K^{\bar\sigma\sigma}\left(\xi + i\frac{\pi}{2}\right) e^{-\xi/2} \sinh^2\frac{\theta_1-\theta_2}{2}}{\prod_i \cosh\frac{\xi-\theta_i}{2} \cosh\frac{\xi+\theta_i}{2}} \right]. \quad \text{(C43)}$$

We note that after analytic continuation $\tau \to it + \delta$ and Fourier transformation $t \to E$, the exponential factor $e^{-\Delta\tau(\sum_i \cosh\theta_i + \cosh\xi)}$ results in a vanishing of N_{21} for energies $E < 3\Delta$.

The final term we wish to evaluate explicitly is the disconnected piece of C_{14}. Considering first $f_\sigma = -1$ and keeping in mind that we have restricted ourselves to the LEP, we can start with

$$C_{14} = \frac{1}{2} \int_{-\infty}^{\infty} \frac{d\xi_1 d\xi_2}{(2\pi)^2} \frac{d\theta}{2\pi} K^{-+}(\xi_1) K^{-+}(\xi_2) e^{\frac{\Delta}{v_s} r\cosh\theta} \times e^{2\frac{\Delta}{v_s} x_2 \sum_i \cosh\xi_i} e^{i\Delta\tau\sinh\theta} \langle 0|e^{\frac{i}{2}\bar\phi_s}|\theta\rangle_+ \times {}^+\langle\theta|e^{\frac{i}{2}\bar\phi_s}|-\xi_1,\xi_1,-\xi_2,\xi_2\rangle_{-+-+}. \quad \text{(C44)}$$

In the second matrix element we keep only the disconnected piece:

$$\begin{aligned} &{}^+\langle\theta|e^{\frac{i}{2}\bar\phi_s}|-\xi_1,\xi_1,-\xi_2,\xi_2\rangle_{-+-+} \\ &= 2\pi\delta(\theta-\xi_1)\langle 0|e^{\frac{i}{2}\bar\phi_s}|-\xi_1,-\xi_2,\xi_2\rangle_{--+} \\ &\quad + 2\pi\delta(\theta-\xi_2)\langle 0|e^{\frac{i}{2}\bar\phi_s}|-\xi_1,\xi_1,-\xi_2\rangle_{-+-} + \cdots \end{aligned} \quad \text{(C45)}$$

In the resulting term C^0_{14} we can shift the contour of integration, $\xi_1 \to \xi_1 + i\pi/2$, to obtain

$$C^0_{14} = -\frac{Z_1}{\sqrt{2}} e^{-i\frac{\pi}{4}} \int_{-\infty}^{\infty} \frac{d\xi_1 d\xi_2}{(2\pi)^2} K^{\sigma\bar\sigma}\left(\xi_1 + i\frac{\pi}{2}\right) \times K^{\sigma\bar\sigma}(\xi_2) \frac{e^{(\xi_1+\xi_2)/2}}{\cosh\xi_2} \frac{e^{\xi_1} + ie^{\xi_2}}{e^{\xi_1+\xi_2} - i} \times e^{2i\frac{\Delta}{v_s} R\sinh\xi_1} e^{2\frac{\Delta}{v_s} x_2 \cosh\xi_2} e^{-\Delta\tau\cosh\xi_1}. \quad \text{(C46)}$$

In the last step we have assumed that no boundary bound states exist (see the following). Finally, we mention that the next term, C^0_{34}, equals C^0_{14} with the coordinates x_1 and x_2 interchanged. These two terms together yield N_{02}.

The remaining two terms, N_{12} and N_{03}, discussed in Sec. IV C, follow from $C^1_{14} + C^1_{34} + C^1_{54}$ and $C^0_{16} + C^0_{36} + C^0_{56}$, respectively.

5. Boundary bound states

As already discussed, the general Dirichlet boundary conditions $\Phi_s(0) = \Phi_s^0 \neq 0$ can result in the appearance of a boundary bound state. If $K_s^2\pi < \Phi_s^0 < \pi$, the boundary reflection amplitude $K^{-+}(\xi)$ has a pole in the physical strip $0 \leqslant \Im\mathrm{m}\,\xi \leqslant \pi/2$ located at[46,55] $\xi = i(\pi - \Phi_s^0)/(2 - 2K_s^2)$. In contrast, $K^{+-}(\xi)$ is analytic in the physical strip but has a pole for $-\pi/2 \leqslant \Im\mathrm{m}\,\xi \leqslant 0$. We write the respective residues as

$$i\,\mathrm{Res}[K^{\mp\pm}(\xi), \xi = \pm i\gamma] = B \geqslant 0, \quad \gamma = \frac{\pi - \Phi_s^0}{2 - 2K_s^2}, \quad \text{(C47)}$$

where B depends on K_s only. We have checked the sign of B by performing an explicit mode expansion at the LEP as well as studying the spectral function of the correlator $\langle 0_b|\, e^{-i\alpha\Phi_s'(\tau,R)}\, e^{i\alpha\Phi_s'(0,R)}\, |0_b\rangle$ (for which the relevant form factors were obtained in Ref. 67).

In the presence of a boundary bound state the poles of $K^{\mp\pm}(\xi)$ will contribute whenever we shift the contour of integration $\xi \to \xi \pm i\pi/2$ in a given term in the form-factor expansion, Eq. (C30). The leading term of this type is obtained from Eq. (C38), which yields Eq. (41) by a straightforward calculation. The subleading term can be obtained similarly

from C^0_{14} and C^0_{34}. At the LEP it is given by ($B = -2\cos\Phi^0_s$, $\pi/2 \leqslant \Phi^0_s \leqslant \pi$)

$$\Theta\left(\Phi^0_s - \frac{\pi}{2}\right) \delta_{\sigma\downarrow}\, Z_1\sqrt{8}\, e^{-\frac{\mathrm{i}}{2}\Phi^0_s} \cos\Phi^0_s\, e^{-2\frac{\Delta}{v_s} R\cos\Phi^0_s}\, e^{-\Delta\tau\sin\Phi^0_s} \times \int_{-\infty}^{\infty} \frac{d\xi}{2\pi} \frac{K^{\sigma\bar\sigma}(\xi)}{\cosh\xi} \frac{\cosh\left(\frac{\xi}{2} + \frac{\mathrm{i}}{2}\Phi^0_s\right)}{\sinh\left(\frac{\xi}{2} - \frac{\mathrm{i}}{2}\Phi^0_s\right)} e^{\xi/2}\, e^{2\frac{\Delta}{v_s} x_2 \cosh\xi}. \tag{C48}$$

APPENDIX D: FOURIER TRANSFORMATION OF THE LDOS

We calculate the auxiliary function

$$I(\omega,k) = \int_{-\infty}^{0} dR \int_{-\infty}^{\infty} dt\, \frac{e^{\mathrm{i}(\omega t - kR)}}{(v_c\tau - 2\mathrm{i}R)^a} \times \frac{1}{(v_c\tau + 2\mathrm{i}R)^b} \left(\frac{2R}{v_c\tau}\right)^{2c} \Bigg|_{\tau\to \mathrm{i}t+\delta} \tag{D1}$$

$$= \int_{-\infty}^{0} dR \int_{-\infty}^{\infty} dt\, \frac{e^{\mathrm{i}(\omega t - kR)}}{(v_c t - 2R - \mathrm{i}\delta)^a} \times \frac{(-\mathrm{i})^{a+b+2c}}{(v_c t + 2R - \mathrm{i}\delta)^b} \left(\frac{2R}{v_c t - \mathrm{i}\delta}\right)^{2c}, \tag{D2}$$

where $v_c, a, b, c \in \mathbb{R}$, $v_c > 0$, $a + b < 2$, and $c > -1/2$. We substitute $R \to -R$ and $t \to -t$, introduce $s = v_c t/2R$ and $\eta \to 0+$, and perform the resulting R integral (3.381.4 in Ref. 63), which yields

$$I(\omega,k) = -\frac{e^{\mathrm{i}\pi(a+b-c)}\,\Gamma(2-a-b)}{2^{a+b-1}\, v_c} \times \int_{-\infty}^{\infty} ds\, \frac{\left(\frac{2\omega}{v_c}s - k - \mathrm{i}\eta\right)^{a+b-2}}{(s-1+\mathrm{i}\delta)^a\,(s+1+\mathrm{i}\delta)^b\,(s+\mathrm{i}\delta)^{2c}}. \tag{D3}$$

For $\omega < 0$ the integrand has all its branch points in the lower half-plane and the integral over s vanishes as long as $c > -1/2$. Hence we find ($s_0 = v_c k/2\omega$)

$$I(\omega,k) = -\Theta(\omega)\,\Gamma(2-a-b) \frac{e^{\mathrm{i}\pi(a+b-c)}\,\omega^{a+b-2}}{2\, v_c^{a+b-1}} \times \int_{-\infty}^{\infty} ds\, \frac{(s - s_0 - \mathrm{i}\eta)^{a+b-2}}{(s-1+\mathrm{i}\delta)^a\,(s+1+\mathrm{i}\delta)^b\,(s+\mathrm{i}\delta)^{2c}}. \tag{D4}$$

First, consider the case $k < 0$. The numerator of the integrand has a branch point at $s = s_0 + \mathrm{i}\eta$ in the upper half-plane. We place the cut running from $-\infty + \mathrm{i}\eta$ to $s_0 + \mathrm{i}\eta$ with constant imaginary part (see Fig. 14). Now we deform the contour of integration and rewrite the integration above the cut as integration below the cut using

$$\int_{-\infty}^{\infty} ds\, (s - s_0 - \mathrm{i}\eta)^{a+b-2}\, g(s) = \int_{-\infty}^{s_0} ds\, (s - s_0 - \mathrm{i}\eta)^{a+b-2}\, g(s)\,[1 - e^{2\pi\mathrm{i}(a+b)}]. \tag{D5}$$

Assuming $1 < a + b$ and substituting $s = s_0/t$, this yields, for the integral in Eq. (D4),

$$-2\mathrm{i}\,\sin[\pi(a+b)]\,|s_0|^{a+b-1} \times \int_0^1 dt\, \frac{t^{2c}\,(1-t)^{a+b-2}}{(s_0 - t + \mathrm{i}\delta)^a\,(s_0 + t + \mathrm{i}\delta)^b\,(s_0 + \mathrm{i}\delta)^{2c}}. \tag{D6}$$

Finally, using (recall $s_0 < 0$, $\delta = 0+$)

$$(s_0 - t + \mathrm{i}\delta)^{-a} = \{s_0[1 - (1/s_0 + \mathrm{i}\delta)t]\}^{-a} = |s_0|^{-a}\, e^{-\mathrm{i}\pi a}\,[1 - (1/s_0 + \mathrm{i}\delta)t]^{-a}, \tag{D7}$$

$$(s_0 + t + \mathrm{i}\delta)^{-b} = \{s_0[1 + (1/s_0 - \mathrm{i}\delta)t]\}^{-b} = |s_0|^{-b}\, e^{-\mathrm{i}\pi b}[1 + (1/s_0 - \mathrm{i}\delta)t]^{-b}, \tag{D8}$$

$$(s_0 + \mathrm{i}\delta)^{-2c} = |s_0|^{-2c}\, e^{-2\pi\mathrm{i}c}, \tag{D9}$$

as well as $e^{-2\pi\mathrm{i}c}/|s_0|^{2c+1} = -(1/s_0 - \mathrm{i}\delta)^{2c+1}$ and $\Gamma(z)\Gamma(1-z) = \pi/\sin(\pi z)$, we obtain

$$I(\omega,k<0) = \frac{\pi\,\Theta(\omega)\,e^{-\mathrm{i}\frac{\pi}{2}(2c-1)}}{\Gamma(a+b-1)} \frac{\omega^{a+b-2}}{v_c^{a+b-1}} \left(\frac{1}{s_0} - \mathrm{i}\delta\right)^{2c+1} \times \int_0^1 dt \frac{t^{2c}(1-t)^{a+b-2}}{[1-(1/s_0+\mathrm{i}\delta)t]^a[1+(1/s_0-\mathrm{i}\delta)t]^b}. \tag{D10}$$

For $k > 0$ we place the cut as shown in Fig. 14. Performing the same steps as above we find

$$I(\omega,k>0) = \frac{\pi\,\Theta(\omega)\,e^{-\mathrm{i}\frac{\pi}{2}(2c-1)}}{\Gamma(a+b-1)} \frac{\omega^{a+b-2}}{v_c^{a+b-1}} \left(\frac{1}{s_0} + \mathrm{i}\delta\right)^{2c+1} \times \int_0^1 dt\, \frac{t^{2c}\,(1-t)^{a+b-2}}{[1-(1/s_0-\mathrm{i}\delta)t]^a\,[1+(1/s_0+\mathrm{i}\delta)t]^b}. \tag{D11}$$

We can write Eqs. (D10) and (D11) together as

$$I(\omega,k) = \frac{\pi\,\Theta(\omega)\,e^{-\mathrm{i}\frac{\pi}{2}(2c-1)}\,\Gamma(2c+1)}{\Gamma(a+b+2c)} \frac{\omega^{a+b-2}}{v_c^{a+b-1}}\, u^{2c+1} \times F_1(2c+1,a,b,a+b+2c;u^*,-u), \tag{D12}$$

$$u = \frac{2\omega}{v_c k} + \mathrm{i}\,\mathrm{sgn}(k)\,\delta.$$

Here we have used the integral representation, Eq. (E2), of Appell's hypergeometric function,[49] which is valid for $1 < a + b$. Analytic continuation in the parameters a, b, and c then yields $I(\omega,k)$ for $a + b < 2$ and $c > -1/2$. At $K_c = 1$ one finds $F_1(2c+1,a,b,a+b+2c;u^*,-u) = F_1(1,1/2,0,1/2;u^*,-u) = 1/(1-u^*)$.

In the same way one can show

$$\int_{-\infty}^{0} dR \int_{-\infty}^{\infty} dt\, \frac{e^{\mathrm{i}(\omega t - kR)}}{(v_c t - 2R - \mathrm{i}\delta)^c} \times \frac{(-\mathrm{i})^{a+b+2c}}{(v_c t + 2R - \mathrm{i}\delta)^c} \frac{(2R)^{2c}}{(v_c t - \mathrm{i}\delta)^{a+b}}$$

$$= \pi\,\Theta(\omega)\,e^{-\mathrm{i}\frac{\pi}{2}(2c-1)} \frac{\omega^{a+b-2}}{v_c^{a+b-1}} \frac{\Gamma(a+b+1)}{\Gamma(2a+2b)} \times u^{2c+1}\, F_1(a+b+1,c,c,2a+2b;u^*,-u),$$

$$u = \frac{2\omega}{v_c k} + \mathrm{i}\,\mathrm{sgn}(k)\,\delta, \tag{D13}$$

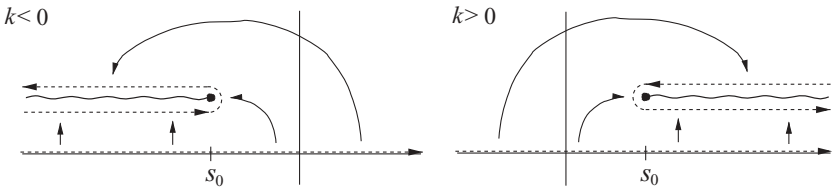

FIG. 14. Branch cut and deformation of the contour of integration used for $k < 0$ and $k > 0$, respectively.

as well as ($A > 0$)

$$\int_{-\infty}^{0} dR \int_{-\infty}^{\infty} dt \, \frac{e^{\mathrm{i}(\omega t - kR)}}{\left(v_c t - 2R - \mathrm{i}\delta\right)^a} \frac{(-\mathrm{i})^{a+b+2c} \, e^{AR}}{\left(v_c t + 2R - \mathrm{i}\delta\right)^b} \left(\frac{2R}{v_c t - \mathrm{i}\delta}\right)^{2c}$$
$$= \frac{\pi \, \Theta(\omega) \, e^{-\mathrm{i}\frac{\pi}{2}(2c-1)}}{\omega^{2-a-b} \, v_c^{a+b-1}} \frac{\Gamma(2c+1)}{\Gamma(a+b+2c)} \left(\frac{2\omega}{v_c k} + \mathrm{i}\,\mathrm{sgn}(k)\,\delta\right)^{2c+1}$$
$$\times F_D^{(3)}\left(2c+1, a, b, 2c, a+b+2c; \frac{2\omega}{v_c k} - \mathrm{i}\frac{A}{k}, -\frac{2\omega}{v_c k} - \mathrm{i}\frac{A}{k}, -\mathrm{i}\frac{A}{k}\right), \tag{D14}$$

where $F_D^{(3)}$ denotes Lauricella's hypergeometric function of three variables (see Appendix E). For $a = 1/2$ and $b = c = 0$, Eq. (D14) simplifies to $2\mathrm{i}\sqrt{\pi v_c}\Theta(\omega)/\sqrt{\omega}/(v_c k - 2\omega + \mathrm{i}v_c A)$.

APPENDIX E: HYPERGEOMETRIC FUNCTION OF SEVERAL VARIABLES

Hypergeometric series of several variables were first studied by Lauricella.[56] They are defined by

$$F_D^{(n)}(\alpha, \beta_1, \ldots, \beta_n, \gamma; z_1, \ldots, z_n)$$
$$= \sum_{m_1,\ldots,m_n=0}^{\infty} \frac{(\alpha)_{m_1+\cdots+m_n} \, (\beta_1)_{m_1} \cdots (\beta_n)_{m_n}}{(\gamma)_{m_1+\cdots+m_n}} \frac{z_1^{m_1} \cdots z_n^{m_n}}{m_1! \cdots m_n!},$$
$$|z_i| < 1. \tag{E1}$$

The special cases[49] $n = 1$ and $n = 2$ are Gauss hypergeometric function, $F_D^{(1)} = F(\alpha, \beta; \gamma; z)$, and Appell's hypergeometric function, $F_D^{(2)} = F_1(\alpha, \beta_1, \beta_2, \gamma; z_1, z_2)$, respectively. The function $F_D^{(n)}$ possesses the Euler-type integral representation,[49,68]

$$F_D^{(n)}(\alpha, \beta_1, \ldots, \beta_n, \gamma; z_1, \ldots, z_n)$$
$$= \frac{\Gamma(\gamma)}{\Gamma(\alpha)\,\Gamma(\gamma - \alpha)}$$
$$\times \int_0^1 dt \, \frac{t^{\alpha-1}(1-t)^{\gamma-\alpha-1}}{(1 - z_1 t)^{\beta_1} \cdots (1 - z_n t)^{\beta_n}},$$
$$\mathfrak{Re}\,\alpha > 0, \quad \mathfrak{Re}\,(\gamma - \alpha) > 0. \tag{E2}$$

Furthermore, the following relations hold:[49,56]

$$F_D^{(n)}(\alpha, \beta_1, \ldots, \beta_n, \gamma; z_1, \ldots, z_n)$$
$$= (1 - z_1)^{-\beta_1} \cdots (1 - z_n)^{-\beta_n}$$
$$\times F_D^{(n)}\left(\gamma - \alpha, \beta_1, \ldots, \beta_n, \gamma; \frac{z_1}{z_1 - 1}, \ldots, \frac{z_n}{z_n - 1}\right), \tag{E3}$$

$$F_1(\alpha, \beta_1, \beta_2, \gamma; 1, 1) = \frac{\Gamma(\gamma)\,\Gamma(\gamma - \alpha - \beta_1 - \beta_2)}{\Gamma(\gamma - \alpha)\,\Gamma(\gamma - \beta_1 - \beta_2)}$$
$$\text{for} \quad \gamma \neq 0, -1, -2, \ldots \quad \text{and} \quad \gamma > \alpha + \beta_1 + \beta_2. \tag{E4}$$

APPENDIX F: PROPERTIES OF $N_\sigma^>(E, 2\mathbf{k}_F + \mathbf{q})$

To analyze the dispersing features and singularities of Eq. (26), we first note that $F_1(2c+1, a, b, a+b+2c; u^*, -u)$ possesses singularities at $u = \pm 1$.

Let us first study $N_1^>$. The integrand has singularities at

$$\text{(i)} \quad E - \Delta\cosh\theta = 0, \quad \text{(ii)} \quad 2(E - \Delta\cosh\theta) = \pm v_c q. \tag{F1}$$

Inserting (i) into (ii) immediately yields a feature at $q = 0$. Using Eqs. (E3) and (E4), one can extract the q dependence $(v_c q)^{a+b-2c-1}$ to obtain Eq. (29). On the other hand, (i) will be stationary at $\theta \approx 0$. Inserting this into (ii) directly yields the dispersion relation, Eq. (30). The suppression of the dispersing peak for $q < 0$ follows from the relative strength of the singularities at $u = \pm 1$.

In the same way the integrand in $N_2^>$ has singularities at

$$\text{(i)} \quad E - \Delta\cosh\theta = 0,$$
$$\text{(iii)} \quad 2v_s(E - \Delta\cosh\theta) = \pm v_c(v_s q - 2\Delta\sinh\theta). \tag{F2}$$

Inserting (i) into (iii) directly yields the dispersion relation, Eq. (31). Furthermore, we can rewrite (iii) as

$$\text{(iv)} \quad \frac{E}{\Delta} \mp \frac{v_c q}{2\Delta} = \cosh\theta \mp \frac{v_c}{v_s}\sinh\theta. \tag{F3}$$

If and only if $v_c < v_s$, the right-hand side of (iv) becomes stationary at $\theta = \tilde{\theta} = \pm\mathrm{arcosh}(v_s/\sqrt{v_s^2 - v_c^2})$. In principle, this leads to the relation, Eq. (32), for arbitrary q. However, this dispersing feature exists only when $-\mathrm{arcosh}(\frac{E}{\Delta}) \leqslant \tilde{\theta} \leqslant \mathrm{arcosh}(\frac{E}{\Delta})$. Together with Eq. (32), this yields the condition $q_0 \leqslant |q|$.

Finally, to prove Eq. (45) we use that $F_D^{(3)}(2c+1, a, b, 2c, a+b+2c; u_3^*, -u_3, -u_3')$ is regular as $E \to E_{\mathrm{bbs}}+$, which directly yields $\alpha = 1 - a - b - 2c = 1 - 1/(2K_c^2)$.

*Correspondence author. schuricht@physik.rwth-aachen.de

[1] T. W. Odom, J.-L. Huang, and C. M. Lieber, J. Phys. Condens. Matter **14**, R145 (2002).

[2] C. Howald, P. Fournier, and A. Kapitulnik, Phys. Rev. B **64**, 100504(R) 2001.

[3] J. E. Hoffman, K. McElroy, D.-H. Lee, K. M. Lang, H. Eisaki, S. Uchida, and J. C. Davis, Science **297**, 1148 (2002); K. McElroy, R. W. Simmonds, J. E. Hoffman, D.-H. Lee, J. Orenstein, H. Eisaki, S. Uchida, and J. C. Davis, Nature **422**, 592 (2003); C. Howald, H. Eisaki, N. Kaneko, M. Greven, and A. Kapitulnik, Phys. Rev. B **67**, 014533 (2003); M. Vershinin, S. Misra, S. Ono, Y. Abe, Y. Ando, and A. Yazdani, Science **303**, 1995 (2004).

[4] Y. Kohsaka, C. Taylor, K. Fujita, A. Schmidt, C. Lupien, T. Hanaguri, M. Azuma, M. Takano, H. Eisaki, H. Takagi, S. Uchida, and J. C. Davis, Science **315**, 1380 (2007).

[5] O. Fischer, M. Kugler, I. Maggio-Aprile, C. Berthod, and C. Renner, Rev. Mod. Phys. **79**, 353 (2007).

[6] A. Fang, N. Ru, I. R. Fisher, and A. Kapitulnik, Phys. Rev. Lett. **99**, 046401 (2007).

[7] R. Wiesendanger, H. J. Güntherrodt, G. Güntherrodt, R. J. Gambino, and R. Ruf, Phys. Rev. Lett. **65**, 247 (1990); R. Wiesendanger, I. V. Shvets, D. Bürgler, G. Tarrach, H. J. Güntherrodt, J. M. D. Coey, and S. Gräser, Science **255**, 583 (1992); S. Heinze, M. Bode, A. Kubetzka, O. Pietzsch, X. Nie, S. Blügel, and R. Wiesendanger, *ibid.* **288**, 1805 (2000).

[8] S. Eggert, Phys. Rev. Lett. **84**, 4413 (2000); P. Kakashvili, H. Johannesson, and S. Eggert, Phys. Rev. B **74**, 085114 (2006); I. Schneider, A. Struck, M. Bortz, and S. Eggert, Phys. Rev. Lett. **101**, 206401 (2008); M. Guigou, T. Martin, and A. Crepieux, Phys. Rev. B **80**, 045420 (2009); I. Schneider and S. Eggert, Phys. Rev. Lett. **104**, 036402 (2010).

[9] S. A. Kivelson, I. P. Bindloss, E. Fradkin, V. Oganesyan, J. M. Tranquada, A. Kapitulnik, and C. Howald, Rev. Mod. Phys. **75**, 1201 (2003).

[10] A. Polkovnikov, M. Vojta, and S. Sachdev, Phys. Rev. B **65**, 220509 (2002); Q.-H. Wang and D.-H. Lee, *ibid.* **67**, 020511 (2003).

[11] D. Podolsky, E. Demler, K. Damle, and B. I. Halperin, Phys. Rev. B **67**, 094514 (2003).

[12] C. L. Kane and M. P. A. Fisher, Phys. Rev. Lett. **68**, 1220 (1992); Phys. Rev. B **46**, 15233 (1992).

[13] M. Grioni, S. Pons, and E. Frantzeskakis, J. Phys. Condens. Matter **21**, 023201 (2009), and references therein.

[14] C. Bourbonnais and D. Jerome, in *Advances in Synthetic Metals, Twenty Years of Progress in Science and Technology*, edited by P. Bernier, S. Lefrant, and G. Bidan (Elsevier, New York, 199), p. 206; T. Giamarchi, Chem. Rev. **104**, 5037 (2004), and references therein; A. Schwartz, M. Dressel, G. Grüner, V. Vescoli, L. Degiorgi, and T. Giamarchi, Phys. Rev. B **58**, 1261 (1998).

[15] I. A. Zaliznyak, H. Woo, T. G. Perring, C. L. Broholm, C. D. Frost, and H. Takagi, Phys. Rev. Lett. **93**, 087202 (2004); B. J. Kim, H. Koh, E. Rotenberg, S.-J. Oh, H. Eisaki, N. Motoyama, S. Uchida, T. Tohyama, S. Mackawa, Z.-X. Shen, and C. Kim, Nat. Phys. **2**, 397 (2006); T. E. Kidd, T. Valla, P. D. Johnson, K. W. Kim, G. D. Gu, and C. C. Homes, Phys. Rev. B **77**, 054503 (2008).

[16] J. W. G. Wildöer, L. C. Venema, A. G. Rinzler, R. E. Smalley, and C. Dekker, Nature **391**, 59 (1998); L. C. Venema, J. W. Janssen, M. R. Buitelaar, J. W. G. Wildöer, S. G. Lemay, L. P. Kouwenhoven, and C. Dekker, Phys. Rev. B **62**, 5238 (2000); P. M. Singer, P. Wzietek, H. Alloul, F. Simon, and H. Kuzmany, Phys. Rev. Lett. **95**, 236403 (2005).

[17] S. Notbohm, P. Ribeiro, B. Lake, D. A. Tennant, K. P. Schmidt, G. S. Uhrig, C. Hess, R. Klingeler, G. Behr, B. Büchner, M. Reehuis, R. I. Bewley, C. D. Frost, P. Manuel, and R. S. Eccleston, Phys. Rev. Lett. **98**, 027403 (2007).

[18] P. Chudzinski, M. Gabay, and T. Giamarchi, New J. Phys. **11**, 055059 (2009).

[19] E. Arrigoni, E. Fradkin, and S. A. Kivelson, Phys. Rev. B **69**, 214519 (2004); E. W. Carlson, V. J. Emery, S. A. Kivelson, and D. Orgad, in *The Physics of Superconductors*, edited by K. H. Bennemann and J. B. Ketterson (Springer, Berlin, 2004), Vol. II; R. M. Konik, F. H. L. Essler, and A. M. Tsvelik, Phys. Rev. B **78**, 214509 (2008).

[20] D. Schuricht, F. H. L. Essler, A. Jaefari, and E. Fradkin, Phys. Rev. Lett. **101**, 086403 (2008).

[21] P. K. Mitter and P. H. Weisz, Phys. Rev. D **8**, 4410 (1973); D. Gross and A. Neveu, *ibid.* **10**, 3235 (1974); R. Dashen and Y. Frishman, *ibid.* **11**, 2781 (1975).

[22] F. H. L. Essler, H. Frahm, F. Göhmann, A. Klümper, and V. E. Korepin, *The One–Dimensional Hubbard Model* (Cambridge University Press, Cambridge, 2005).

[23] T. Holstein, Ann. Phys. **8**, 325 (1959).

[24] A. J. Heeger, S. Kivelson, J. R. Schrieffer, and W.-P. Su, Rev. Mod. Phys. **60**, 781 (1988).

[25] E. Fradkin and J. E. Hirsch, Phys. Rev. B **27**, 1680 (1983).

[26] In Ref. [25], only the half-filled case is discussed. At half-filling, the CDW is commensurate, and due to the existence of an Umklapp operator, the CDW does not slide. The effective field theory is a nonchiral SU(2) Gross-Neveu model. In this regime the system is effectively a Mott insulator. Away from half-filling the CDW slides, as the Umklapp operator is absent (irrelevant), and the effective field theory is a chiral SU(2) Gross-Neveu model that is equivalent to a U(1) Thirring model with two flavors. This model has a continuous chiral symmetry, a consequence of the sliding invariance of the CDW. This is, in fact, the generic description of the low-energy physics of a 1D system with a CDW ground state, regardless of the microscopic origin of this state.

[27] S. White, I. Affleck, and D. J. Scalapino, Phys. Rev. B **65**, 165122 2002.

[28] A. M. Tsvelik, Phys. Rev. B **77**, 073402 (2008).

[29] S. Ghoshal and A. B. Zamolodchikov, Int. J. Mod. Phys. A **9**, 3841 (1994); **9**, E4353 (1994).

[30] A. MacIntyre, J. Phys. A **28**, 1089 (1995); H. Saleur, S. Skorik, and N. P. Warner, Nucl. Phys. B **441**, 421 (1995).

[31] A. Luther and V. J. Emery, Phys. Rev. Lett. **33**, 589 (1974); P. A. Lee, *ibid.* **34**, 1247 (1975).

[32] A. B. Zamolodchikov, Commun. Math. Phys. **55**, 183 (1977).

[33] S. Ghoshal, Int. J. Mod. Phys. A **9**, 4801 (1994).

[34] S. R. White, R. M. Noack, and D. J. Scalapino, Phys. Rev. Lett. **73**, 886 (1994); L. Balents and M. P. A. Fisher, Phys. Rev. B **53**, 12133 (1996); H.-H. Lin, L. Balents, and M. P. A. Fisher, *ibid.* **56**, 6569 (1997); C. Wu, W. V. Liu, and E. Fradkin, *ibid.* **68**, 115104 (2003); D. Controzzi and A. M. Tsvelik, *ibid.* **72**, 035110 (2005); A. M. Tsvelik, e-print arXiv:1004.5092.

[35] H.-H. Lin, L. Balents, and M. P. A. Fisher, Phys. Rev. B **58**, 1794 (1998); R. M. Konik and A. W. W. Ludwig, *ibid.* **64**, 155112 (2001); F. H. L. Essler and R. M. Konik, *ibid.* **75**, 144403 (2007).

[36] M. Fabrizio and A. O. Gogolin, Phys. Rev. B **51**, 17827 (1995); S. Eggert, H. Johannesson, and A. Mattsson, Phys. Rev. Lett.

76, 1505 (1996); S. Eggert, A. E. Mattsson, and J. M. Kinaret, Phys. Rev. B **56**, R15537 (1997); A. E. Mattsson, S. Eggert, and H. Johannesson, *ibid.* **56**, 15615 (1997); P. Lecheminant and E. Orignac, *ibid.* **65**, 174406 (2002).

[37] J. L. Cardy, Nucl. Phys. B **240**, 514 (1984); in *Phase Transitions and Critical Phenomena*, edited by C. Domb and J. L. Lebowitz (Academic Press, London, 1987), Vol. 11.

[38] P. Di Francesco, P. Mathieu, and D. Sénéchal, *Conformal Field Theory* (Springer, New York, 1997).

[39] F. A. Smirnov, *Form Factors in Completely Integrable Models of Quantum Field Theory* (World Scientific, Singapore, 1992).

[40] A. Fring, G. Mussardo, and P. Simonetti, Nucl. Phys. B **393**, 413 (1993); S. Lukyanov, Mod. Phys. Lett. A **12**, 2543 (1997); H. Babujian, A. Fring, M. Karowski, and A. Zapletal, Nucl. Phys. B **538**, 535 (1999); H. Babujian and M. Karowski, *ibid.* **620**, 407 (2002); J. Phys. A **35**, 9081 (2002).

[41] S. Lukyanov, Commun. Math. Phys. **167**, 183 (1995).

[42] S. Lukyanov and A. B. Zamolodchikov, Nucl. Phys. B **607**, 437 (2001).

[43] G. Delfino, J. Phys. A **37**, R45 (2004).

[44] F. H. L. Essler and R. M. Konik, in *From Fields to Strings: Circumnavigating Theoretical Physics (Ian Kogan Memorial Collection)*, edited by M. Shifman, A. Vainshtein, and J. Wheater (World Scientific, Singapore, 2005), Vol. I.

[45] M. Ameduri, R. Konik, and A. LeClair, Phys. Lett. B **354**, 376 (1995); L. Mezincescu and R. I. Nepomechie, Int. J. Mod. Phys. A **13**, 2747 (1998).

[46] P. Mattsson and P. Dorey, J. Phys. A **33**, 9065 (2000).

[47] J.-S. Caux, H. Saleur, and F. Siano, Nucl. Phys. B **672**, 411 (2003).

[48] D. Schuricht and F. H. L. Essler, J. Stat. Mech. (2007) P11004.

[49] A. Erdélyi, ed., *Higher Transcendental Functions* (McGraw-Hill, New York, 1953), Vol. I.

[50] J. Voit, Eur. Phys. J. B **5**, 505 (1998); F. H. L. Essler and A. M. Tsvelik, Phys. Rev. B **65**, 115117 (2002); H. Benthien, F. Gebhard and E. Jeckelmann, Phys. Rev. Lett. **92**, 256401 (2004); T. Ulbricht and P. Schmitteckert, Eur. Phys. Lett. **89**, 47001 (2010).

[51] F. H. L. Essler and A. M. Tsvelik, Phys. Rev. Lett. **90**, 126401 (2003).

[52] V. P. Yurov and Al. B. Zamolodchikov, Int. J. Mod. Phys. A **6**, 3419 (1991).

[53] J. L. Cardy and G. Mussardo, Nucl. Phys. B **410**, 451 (1993); G. Delfino and G. Mussardo, *ibid.* **455**, 724 (1995); G. Delfino and J. L. Cardy, *ibid.* **519**, 551 (1998); D. Controzzi, F. H. L. Essler, and A. M. Tsvelik, Phys. Rev. Lett. **86**, 680 (2001).

[54] A. Kapustin and S. Skorik, J. Phys. A **29**, 1629 (1996); F. H. L. Eßler and H. Frahm, Phys. Rev. B **56**, 6631 (1997).

[55] S. Skorik and H. Saleur, J. Phys. A **28**, 6605 (1995).

[56] G. Lauricella, Rend. Circ. Matem. Palermo **7**, 111 (1893).

[57] F. H. L. Essler and R. M. Konik, Phys. Rev. B **78**, 100403(R) (2008); J. Stat. Mech. (**2009**) P09018.

[58] H. W. J. Blöte, J. L. Cardy, and M. P. Nightingale, Phys. Rev. Lett. **56**, 742 (1986); I. Affleck, *ibid.* **56**, 746 (1986).

[59] P. Abbamonte, G. Blumberg, A. Rusydi, A. Gozar, P. G. Evans, T. Siegrist, L. Venema, H. Eisaki, E. D. Isaacs, and G. A. Sawatzky, Nature **431**, 1078 (2004).

[60] K. Magishi, S. Matsumoto, Y. Kitaoka, K. Ishida, K. Asayama, M. Uehara, T. Nagata, and J. Alimitsu, Phys. Rev. B **57**, 11533 (1998).

[61] C. V. Parker, P. Aynajian, E. H. da Silva Neto, A. Pushp, S. Ono, J. Wen, Z. Xu, G. Gu, and A. Yazdani, Nature (London) **468**, 677 (2010).

[62] A. O. Gogolin, A. A. Nersesyan, and A. M. Tsvelik, *Bosonization and Strongly Correlated Systems* (Cambridge University Press, Cambridge, 1998).

[63] I. S. Gradshteyn and I. M. Ryzhik, *Table of Integrals, Series, and Products* (Academic Press, London, 1980).

[64] Al. B. Zamolodchikov, Int. J. Mod. Phys. A **10**, 1125 (1995).

[65] A. B. Zamolodchikov and Al. B. Zamolodchikov, Ann. Phys. **120**, 253 (1979); L. D. Faddeev, Sov. Sci. Rev. Math. Phys. C **1**, 107 (1980).

[66] V. E. Korepin, Theor. Math. Phys. **41**, 169 (1979).

[67] S. Lukyanov, Mod. Phys. Lett. A **12**, 2543 (1997).

[68] H. Exton, *Handbook of Hypergeometric Integrals: Theory, Applications, Tables, Computer Programs* (Ellis Horwood, Chichester, UK, 1978).